Scottish Universities Environmental Research Centre

SE Asia Agricultural Soils Age Analysis

February 2019

A.J. Cresswell[1], D.C.W. Sanderson[1], P.A. Carling[2], S. Darby[2]

[1] SUERC, East Kilbride, Glasgow
[2] Geography and Environment, University of Southampton

East Kilbride Glasgow G75 0QF Telephone: 01355 223332 Fax: 01355 229898

Summary

The soils of southeast Asia include regionally extensive layers of generally sandy material, in some places 5m or more in depth, observed throughout Vietnam, Cambodia and Thailand, and upland areas of Myanmar and Malaysia, and even the Punjab. Various explanations for the origin of these layers have been proposed, with clarification of their ages and modes of emplacement remaining a significant issue. In many locations, these cover sands overlay a laterite layer containing tektites associated with a 750-800ka old meteorite impact in the region.

Luminescence measurements have been used to date and characterise these sand layers, and in this report such measurements from five locations in Thailand and one site in Vietnam have been reviewed. This suggests that luminescence methods can readily distinguish between two distinct classes of material within these sand layers: 1. Sands with lower luminescence sensitivity and OSL depletion indices with ages in excess of ~50ka (the limit of SAR OSL methods); 2. Sands with high luminescence sensitivity and OSL depletion indices with ages less than 35ka. At four locations in Thailand only the younger material is present, with ages for basal samples of 9-35ka. At the other Thai site (Huai Om) both are present, with the older material in the lower 50cm of the section, and the young material immediately above this giving an age of approximately 30ka. At the site in Vietnam (Hue), there is evidence that the materials have experienced mixing, with some younger material within the older layer. The use of OSL intensities and depletion indices from the Portable OSL reader would be a method of rapidly distinguishing between these two classes of sand in the field.

Dose extension methods have been used to estimate equivalent doses for the older materials. Applied to the younger materials, these give equivalent doses within 20% of the OSL method. For the older materials at Huai Om and Hue these give equivalent doses consistent with an age of 100-150ka, although the data suggest that the traps associated with these measurements have lifetimes of ~10^5 years at environmental temperatures of 25°C, which could significantly underestimate the age of these minerals. Further investigations into trap stability may be useful, including (if possible) collection of samples from equivalent contexts with lower environmental temperatures (eg: at higher altitude).

Contents

List of figures

List of tables

1. Introduction

A significant feature of the soils of southeast Asia is a regionally extensive layer of generally sandy material, in some places 5m or more in depth (eg. Nichol&Nichol 2015, Tamura 1992). These layers are observed throughout Vietnam, Cambodia and Thailand, and also reported from upland areas of Myanmar and Malaysia, and even the Punjab. The origin of this sand layer has been explained as aeolian (loess-like) deposits of late Pleistocene to Holocene age (Boonsener and Tassanasorn, 1983; Sonsuk and Hastings, 1984; Boonsener, 1987, 1991; Hoang Ngoc Ky., 1989, 1994; Udomchoke, 1989; Šibrava, 1993), lacustrine (Dheeradilok, 1987), marine (Nguyen Duc Tam, 1994) or fluvial (De Dapper, 1987) sediments. Bioturbation is known to be relevant to the processes of formation (Williams, 1978; Bishop et al., 1980; Johnson, 1993), and it has been suggested that this layer is a result of termite activity and subsequent degradation of termite mounds (Löffler and Kubiniok, 1991, 1996). Clarification of the cover layer's age and mode of emplacement is a significant issue (Šibrava, 1993).

Luminescence measurements have been shown to have the potential to date and characterise these sand layers. Samples collected from sites in the Khon Kaen area of NE Thailand (Sanderson et.al. 2001) had excellent luminescence properties, with high-luminescence sensitivity quartz producing consistent ages from both Optically Stimulated Luminescence (OSL) and Thermoluminescence (TL), indicating material that had been strongly bleached prior to deposition. Ages down a 2m profile increased from ~10ka to ~35ka, as expected from an aeolian depositional history with a rate of deposition far higher during the colder periods of the last glacial cycle. This conclusion is supported by physical characterisation of materials from this region by Nichol & Nichol (2015). More recently, OSL ages have been derived for the basal layer of these sand deposits in Thailand of 8 and 19ka (Porat 2017). Studies of samples from Hue, Vietnam (Cresswell et.al. 2018a,b), have shown that the corresponding sand layers have significantly lower luminescence sensitivities, with minerals which indicate less bleaching with TL signals registering a residual geological component, and a more complex age-depth relationship. The basal layer of this location shows mixing between material with an age of 14 ± 2 ka and material with an age significantly in excess of 50ka. Further analysis of the older components (Cresswell et.al. 2018b) using thermal transfer approaches indicated that these older components would have ages of 100-125ka, although with evidence that the associated traps may not be stable at environmental temperatures above 25°C.

In many locations, these cover sands overlay a tektite containing laterite layer (Tamura 1992, Nichol&Nichol 2015; Mizera et.al. 2016). These tektites, known as the Muong Nong type after the initial descriptions from samples collected a few km south of Muong Nong, Laos (Lacroix 1935), have been identified and dated from several locations in the region. For example, samples from Muong Nong gave fission track ages of between 610 and 720ka have been measured (Gentner et.al. 1969), from Kemeraj, Thailand, an age of 670 ± 40ka (Gentner et.al. 1969), from Phang Daen, Thailand, ages of 700 and 780ka (Fleischer et.al. 1969), from Kan Luang Dong, Thailand an age of 450ka (Fleischer et.al. 1969), samples from several locations around Khon Kaen give fission track ages of 620-700ka (Tamura 1992). These tektites are considered to be a type of tektite within a range of tektite referred to as Australasian tektites first described by Darwin (1844) from a sample collected in the

Darling River Valley in Australia, with other examples collected during the 19th century from Borneo, Malaysia and Java. The extensive strewn field associated with these and subsequent finds extends from southern China to Tasmania, from the east coast of Australia to the Indian Ocean, with an estimated total mass of tektites ranging from $1x10^{11}$ to $3x10^{13}$ kg (Schmidt et al., 1993). These tektites are associated with a large meteorite impact 750 to 800ka in Indochina within the border area between Thailand, Laos and Cambodia (eg: Koeberl 1992), although no impact crater has been located, or the coastal waters of Vietnam (e.g., Schnetzler et al., 1988).

The work presented here will compare luminescence properties and associated ages for cover sands in different locations in SE Asia (Figure 1.1), from the OSL literature outlined above and three additional locations, to identify any trends or regional commonalities and differences. Within these study areas, extensive studies of tektites have been conducted from samples collected near Khon Kaen (Tamura 1992, Mizera et.al. 2016) and within the Ubon Ratchthani region in the south east of Thailand (Koeberl 1992, Mizera et.al. 2016), with Huai Om also in that region.

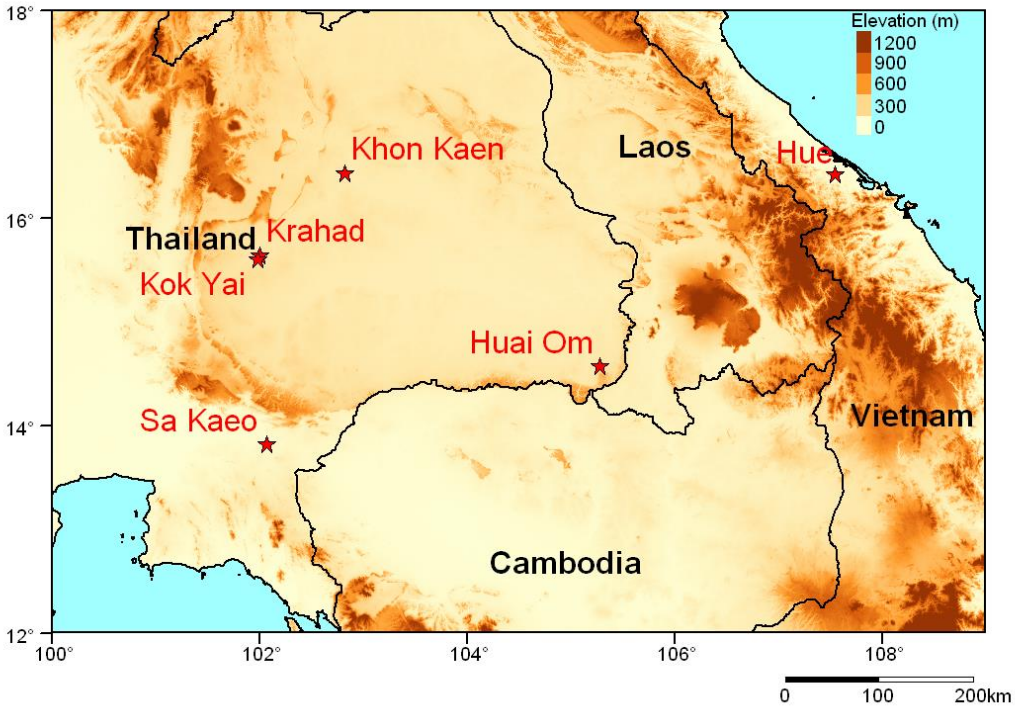

Figure 1.1: Locations of luminescence measurements of cover sands in SE Asia. Khon Kaen was the location of samples reported in Sanderson et.al. 2001. Samples reported in Porat 2017 were collected at Kok Yai and Krahad, and the samples reported by Cresswell et.al. 2018a,b were collected at Hue. Samples from Kok Yai, Huai Om and Sa Kaeo are reported in this work.

2. Methods

2.1. Sampling and sample preparation

Samples were collected by Paul Carling in March 2018 from three locations in Thailand. From Kok Yai two tube samples were collected for dating, one from the impact associated blast gravel layer and one from a position 1m above this. From Sa Kaeo a tube sample was collected from the blast gravel layer. From Huai Om a tube sample was collected from the blast gravel layer, and two profiles of stub samples were also collected. The first profile was of six samples in the lowest unit of the deposit, and three controls from each of the three lowest units. The control samples were bleached in the field to remove luminescence signals. The second profile of 19 samples represent a fuller profile, however the sampling interval was incomplete due to difficulty penetrating gravelly sediments which were sometimes indurated, and a few may have been partially exposed to light. The second profile is given lowest priority for analysis.

Each sample was given a laboratory (SUTL) reference code upon receipt at SUERC, as summarised in Table 2.1.

Table 2.1: Summary of samples and SUERC laboratory reference codes

SUERC code	Depth (cm)	Description
SUTL2986	Six stub samples and three control samples from Huai Om for environmental profiling. Depths given relative to uppermost sample	
SUTL2986/1	210	OM-1, basal layer
SUTL2986/2	200	OM-2
SUTL2986/3	190	OM-3
SUTL2986/4	180	OM-4
SUTL2986/5	170	OM-5
SUTL2986/6	160	OM-6
SUTL2986/7	160	HO-1 (control)
SUTL2986/8	110	HO-2 (control)
SUTL2986/9	0	HO-3 (control)
SUTL2987	Dating sample from impact associated blast gravel layer at Kok Yai	
SUTL2988	Dating sample from 1 m above blast gravel layer at Kok Yai	
SUTL2989	Dating sample from blast gravel layer at Huai Om	
SUTL2990	Dating sample from blast gravel layer at Sa Kaeo (SK3 (C))	
SUTL2991	Nineteen stub samples from Huai Om. Low priority for analysis	

2.2. Portable OSL Measurements

The profile samples (SUTL2986), excluding the bleached control samples, were appraised using the SUERC portable OSL reader, following an interleaved sequence of system dark count (background), infra-red stimulated luminescence (IRSL) and OSL, similar to that described by Sanderson and Murphy (2010). This method allows for the calculation of IRSL and OSL net signal intensities, depletion indices and IRSL:OSL ratios, which are then used to generate luminescence-depth profiles.

2.3. Laboratory Profile Measurements

Simple calibrated laboratory luminescence screening measurements were undertaken on polymineral and quartz fractions to provide a preliminary assessment of sensitivities and stored dose estimates throughout the Huai Om profile (SUTL2986) and from each of the four dating samples.

2.3.1. Sample preparation

All sample handling and preparation was conducted under safelight conditions in the SUERC luminescence dating laboratories. A small portion of each sample (~2 g) was wet sieved to extract the 90-250 µm grain size fraction. This was subjected to an acid treatment of 1M HCl for 10 minutes, 15% HF for 10 mins and 1M HCl for 10 mins, with the sample washed thoroughly with deionised water between each treatment. Approximately half of the material was retained, washed in acetone to displace water and dried as a polymineral sample. The remaining material was subjected to a further acid treatment of 40% HF for 40 mins and 1M HCl for 10 mins, with the sample washed thoroughly with deionised water between each treatment. This fraction was washed in acetone to displace water and dried as a nominal quartz sample.

Clean 10 mm diameter stainless steel discs were prepared with one side sprayed with silicone grease as an adhesive layer, with sample material dispensed as a monolayer onto the central ~5 mm of the disc. For each sample, a pair of polymineral and a pair of quartz discs were dispensed.

2.3.2. Sample Measurements

Luminescence sensitivities (Photon Counts per Gy), sensitivity changes and stored doses (Gy) were evaluated from the paired aliquots of the polymineral and HF-etched quartz fractions, using Risø DA-15 automatic readers equipped with a $^{90}Sr/^{90}Y$ β-source for irradiation, using blue LEDs emitting around 470 nm (OSL) and infrared (laser) diodes emitting around 830 nm (IRSL) for optical stimulation, and a U340 detection filter pack to detect in the region 270-380 nm. For quartz, each measurement was preceded by a pre-heat at 200°C for 10s, with a 30s OSL measurement at 125°C. Measurements were conducted for the natural signal, and following nominal 5 Gy and 50 Gy irradiations, with all measurements accompanied by a nominal 1 Gy test dose. For the polymineral samples, each measurement was preceded by a pre-heat at 200°C for 10s, with a 30s IRSL measurement at 50°C and a TL measurement to 500°C. Measurements were conducted for the natural signal, and following nominal 5 Gy and 50 Gy irradiations. No test dose measurements were included.

2.3.3. Preliminary dose extension evaluation

A single run for four pairs of aliquots of the quartz fraction from the material prepared for profile measurements was run, summarised in Table 2.2, incorporating OSL for a 220°C preheat, followed by TL ramps to 260°C, 280°C, 300°C and 320°C (different temperature for each group) and a 60s isothermal hold, followed by a TT-OSL measurement. This sequence replicates some of the measurements previously

conducted on material from Vietnam confirming that such measurements can be conducted to doses of 1 kGy (Cresswell et.al. 2018b). The measurements conducted here were to confirm that these samples have luminescence characteristics sufficiently similar to the Vietnamese samples that the dose extension method developed for those can be applied to the samples analysed here.

Table 2.2: Exploratory measurements. All steps are common to all sets except steps 3 & 4. The sequence is followed for the natural signal, and then repeated following a 200 Gy dose.

Step	Set A	Set B	Set C	Set D
1	PH 220°C 10s			
2	OSL 60s at 125°C			
3 TL ramp	To 260°C	To 280°C	To 300°C	To 320°C
4 ID	Hold 260°C 60s	Hold 280°C 60s	Hold 300°C 60s	Hold 320°C 60s
5 TTOSL	OSL 60s at 125°C			
6	Thermal treatment 350°C 200s			

2.4. Dating Sample Measurements

The larger dating samples were processed to quantify water content, dose rates and equivalent doses.

2.4.1. Water Content

The outermost material to a depth of 3-5cm was removed from the end of each tube, dried and retained as a bulk material. The tube samples were weighed, saturated with water and re-weighed. Following oven drying at 50°C to constant weight, the actual and saturated water contents were determined as fractions of dry weight. These data were used, together with information on field conditions to determine water contents and an associated water content uncertainty for use in dose rate determination.

2.4.2. Dose Rates

From each of the tube samples, 20 g of the dried material was used in thick source beta counting (TSBC; Sanderson, 1988).

Approximately 20 g of material from the potentially light exposed tube ends was removed from each sample for environmental dose rate determinations. These dried materials were transferred to petri dishes and sealed with epoxy resin for high-resolution gamma spectrometry (HRGS). Each dish was stored for 3 weeks prior to measurement to allow equilibration of ^{222}Rn daughters.

2.4.3. Quartz mineral preparation

Approximately 20 g of material was removed for each tube and processed to obtain sand-sized quartz grains for luminescence measurements. Each sample was wet sieved to obtain the 90-150 and 150-250 μm fractions. The 150-250 μm fractions were

treated with 1 M hydrochloric acid (HCl) for 10 minutes, 10% hydrofluoric acid (HF) for 10 minutes, and 1 M HCl for a further 10 minutes. The HF-etched sub-samples were then centrifuged in sodium polytungstate solutions of ~2.51, 2.58, 2.64, and 2.74 g cm^{-3}, to obtain concentrates of potassium-rich feldspars (2.51-2.58 g cm^{-3}), sodium feldspars (2.58-2.64 g cm^{-3}) and quartz plus plagioclase (2.64-2.74 g cm^{-3}). The selected quartz fraction was then subjected to further HF and HCl washes (40% HF for 40 mins, followed by 1M HCl for 10 mins).

All materials were dried at 50°C and transferred to Eppendorf tubes. The 40% HF-etched, 2.64-2.74 g cm^{-3} 'quartz' 150-250 µm fractions were dispensed to 10 mm stainless steel discs for measurement. 16 aliquots were dispensed for each sample. The purity of these quartz materials was checked using optical microscopy and a Hitachi S-3400N scanning electron microscope (SEM), coupled with an Oxfords Instruments INCA EDX system, to determine approximate elemental concentrations for each sample.

2.4.4. **Equivalent dose determination**

A procedure for equivalent dose determination was developed, modifying the Single Aliquot Regeneration (SAR) procedure to include extended dose measurements. A thermal transfer step, with a TL ramp measurement, isothermal decay and TT-OSL measurement, was included in the natural readout. A standard SAR procedure was then followed to doses of 50 Gy, with higher doses with the thermal transfer steps applied.

Table 2.3: Procedure for combining SAR OSL with dose extension.

Step	Set A	Set B	Set C	Set D
1	Dose (0Gy for natural; regen doses of 10, 20, 30, 40, 50Gy, zero and 10Gy for OSL SAR; regen doses of 50, 100, 200, 500, 1000Gy, zero, & 50Gy for dose extension)			
2 - PH	PH 220°C 10s	PH 240°C 10s	PH 260°C 10s	PH 280°C 10s
3 - OSL	OSL 60s at 125°C (all measurement)			
4 - TL	TL ramp to 260°C (for natural and dose extension)			
5 - ID	Isothermal decay for 30s (for natural and dose extension)			
6 - TTOSL	TT-OSL 60s at 125°C (for natural and dose extension)			
7 - TD	1 Gy Test Dose (for natural and OSL SAR)			
8 - PH	PH 220°C 10s	PH 240°C 10s	PH 260°C 10s	PH 280°C 10s
9 - OSL	OSL 60s at 125°C (for natural and OSL SAR)			
10 - TD	50 Gy Test Dose (for natural and dose extension)			
11 - PH	PH 220°C 10s	PH 240°C 10s	PH 260°C 10s	PH 280°C 10s
12 - OSL	OSL 60s at 125°C (for natural and dose extension)			
13 - TL	TL ramp to 260°C (for natural and dose extension)			
14 - ID	Isothermal decay for 30s (for natural and dose extension)			
15 - TTOSL	TT-OSL 60s at 125°C (for natural and dose extension)			
16	Thermal treatment 350°C 200s (for dose extension)			

3. Results

3.1. Portable OSL measurements

Results of measurements of the six samples in the Huai OM profile are shown in Figure 3.1, and tabulated in the Appendix (Table A.1). The OSL net counts and depletion ratios for the lower five samples are very similar, however the top sample shows a significantly higher value for the photon count and depletion index. The high values of the OSL depletion index are consistent with a significant contribution from sensitive quartz. For the IRSL, the net counts are significantly lower than for the OSL, with the lower sample showing a significantly larger signal.

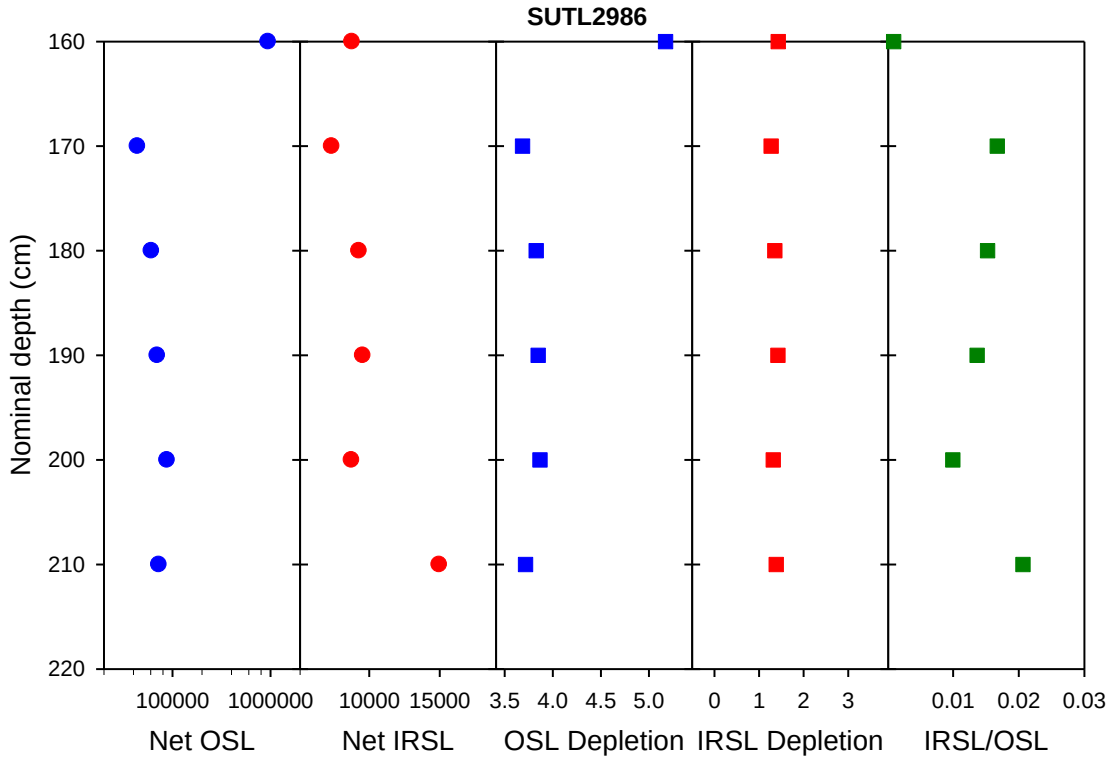

Figure 3.1: Portable OSL measurements for the Huai Om profile (excluding control samples)

3.2. Laboratory Profile Measurements

3.2.1. Huai Om Profile (SUTL2986)

The results of the measurements of all nine samples from the Huai Om profile (including the control samples) are shown in Figure 3.2, and given in the Appendix (Tables A.2-A.5). These samples show very low sensitivity for IRSL on the polymineral phase (<40 counts per Gy), and hence the data for sensitivity change and apparent dose carry substantial uncertainties. The OSL from both quartz and polymineral phases shows higher sensitivity, with the quartz phase sensitivity higher by a factor of typically 3-10. Both fractions show an OSL sensitivity change of approximately 20%, with the polymineral phase increasing sensitivity while the quartz phase sensitivity is reduced. The apparent dose (determined from response to the

50 Gy dose) for the control samples is very close to zero, whereas the apparent doses for the remaining samples are similar (at about 40-60 Gy for the quartz and 200-400 Gy for the polymineral). These apparent doses are consistent for samples where the OSL traps are close to saturation. For sample SUTL2986/6 (at the top of the profile) the OSL sensitivity is very much higher than for the samples below it, which explains the higher net OSL counts observed with the portable reader, and is similar to all three of the control samples. This difference is sensitivity suggests that these six samples are not all from the same depositional unit, despite observations during sampling. The sharp division between sensitivities also suggests minimal mixing between these depositional units. The very high apparent doses for the TL measurements reflect incomplete resetting of the trapped charge centres prior to deposition, the non-zero apparent doses for the control samples indicate that the level of daylight exposure which reset the charge traps accessed by photostimulation has only partially reset the traps accessed by thermostimulation.

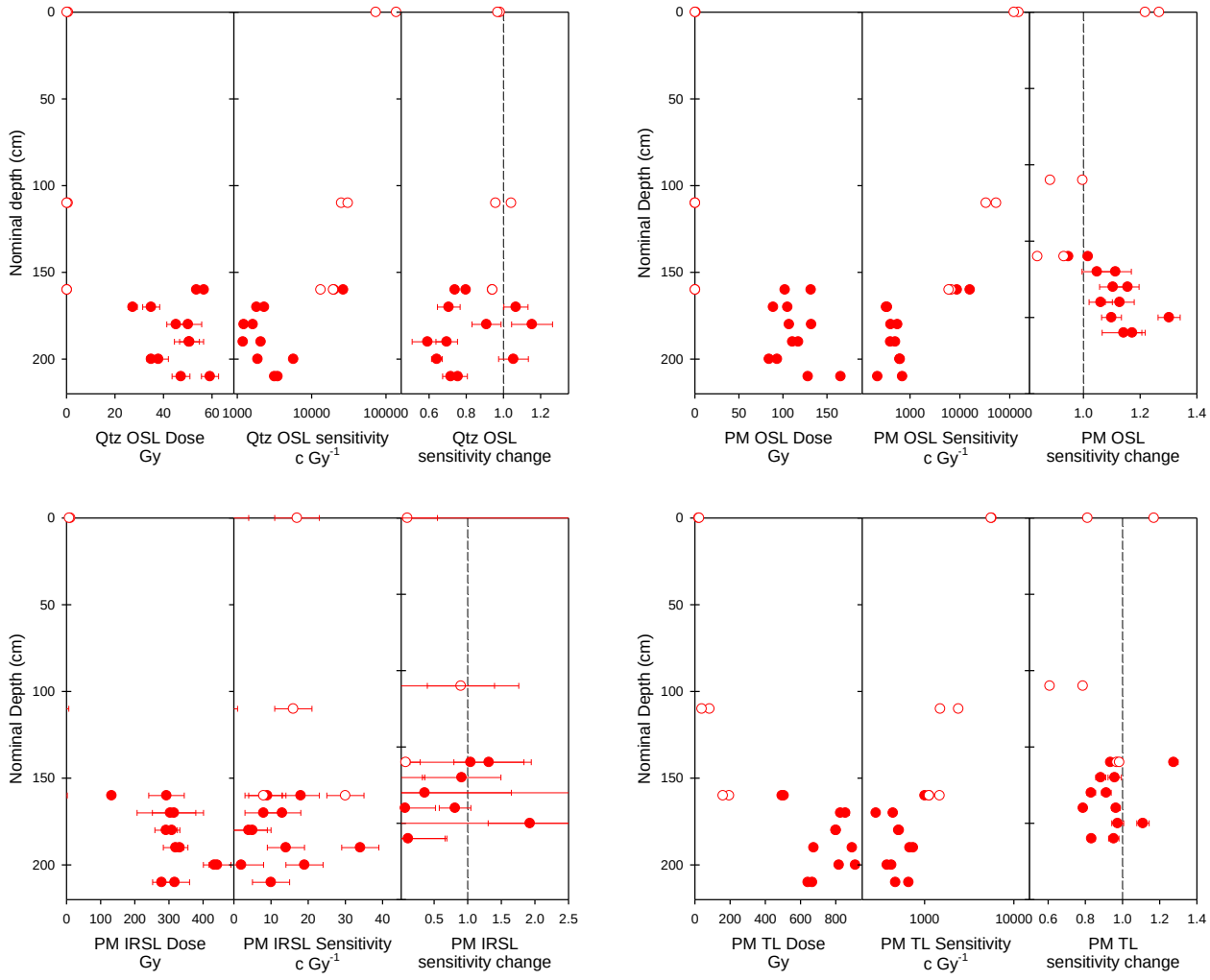

Figure 3.2: Laboratory profiling results from Huai Om profile, open circles indicating the control samples, for the OSL measurements on quartz (top left) and polymineral (top right), IRSL (bottom left) and TL (bottom right) on polymineral grains.

3.2.2. **Tube samples (SUTL2987-2990)**

A small quantity of material from each of the four tube samples was also processed using the profiling procedure. The results of these are shown in Figure 3.3, including the values for SUTL2986/1 which is from the same location as SUTL2989, and also included in Tables A.2-A.5 in the appendix. All samples show very low IRSL sensitivity from the polymineral phases. The data from SUTL2989 are similar to those from SUTL2986/1, whereas the other three samples are markedly different with OSL sensitivities larger by factors of 25-50, and apparent doses <15 Gy in the OSL from both quartz and polymineral and the TL from polymineral phases. The sensitivities of the samples from Kok Yai (SUTL2987-2988) and Sa Kaeo (SUTL2990) are similar to the sensitivities for the upper samples from the Huai Om profile (SUTL2986/6-/9), though with apparent doses that are much lower. The very low apparent doses for the TL measurements imply significant bleaching prior to deposition. These samples show similar characteristics to previously measured cover sands from Khon Kaen in NE Thailand (Sanderson et.al. 2001) and Hue in Vietnam (Cresswell et.al. 2018a).

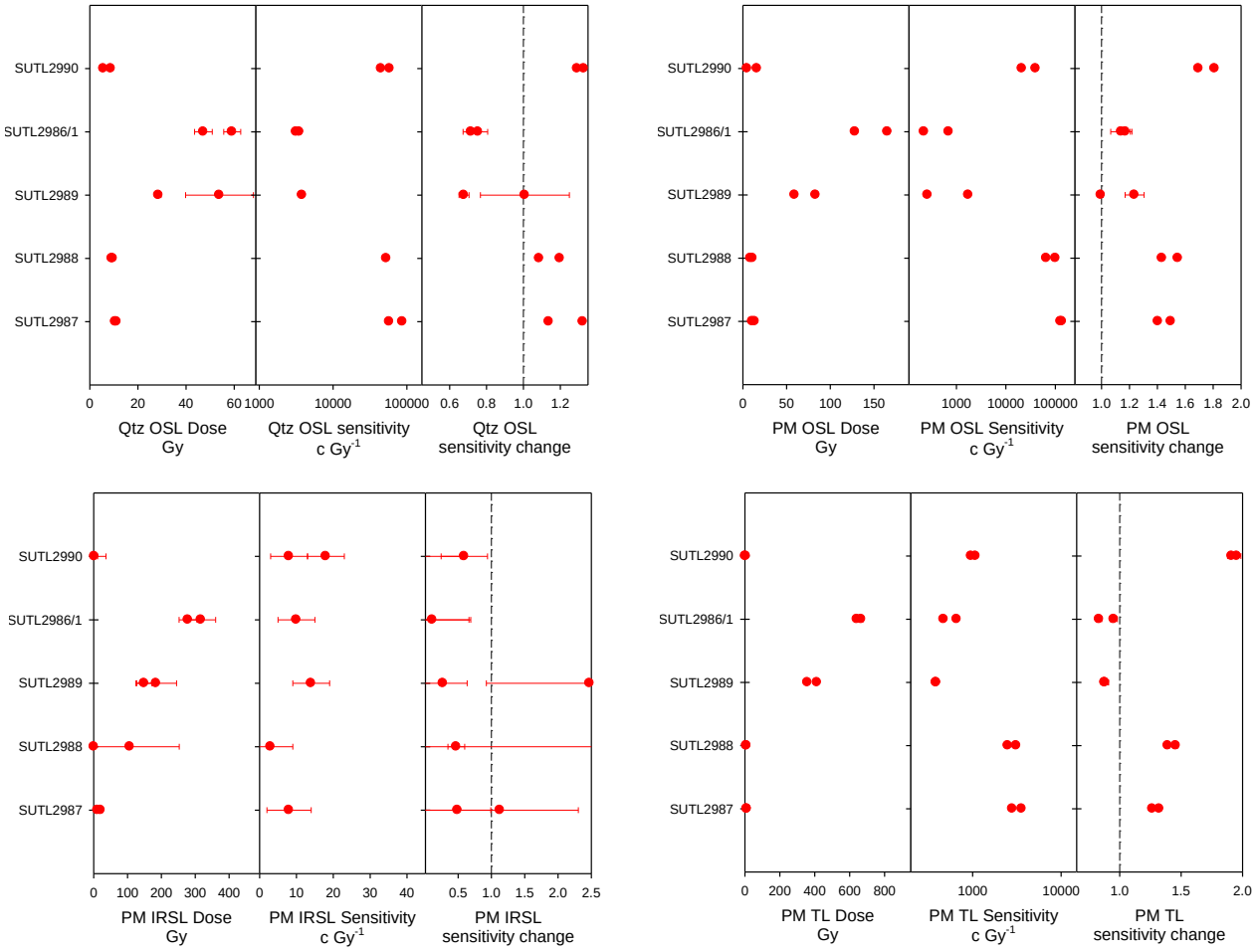

Figure 3.3: Laboratory profiling results from the four tube samples and SUTL2986/1 (equivalent to SUTL2989), for the OSL measurements on quartz (top left) and polymineral (top right), IRSL (bottom left) and TL (bottom right) on polymineral grains.

3.2.3. **Dose extension on profile samples (SUTL2986)**

Sets of aliquots were dispensed for the quartz fraction from SUTL2986/1 (the basal sample) and SUTL2986/6 (the top sample, showing higher sensitivity). A measurement sequence similar to that used for investigation of dose extension on samples from Vietnam (Cresswell et.al. 2018b) was applied to these as described in section 2.3.3, above, to determine whether there are any significant differences in the characteristics of these samples compared to those from Vietnam, and hence whether the SAR procedure developed for the samples from Vietnam would be suitable for these samples.

Integrated counts for the OSL, TL ramp, isothermal decay and TT-OSL for these measurements are given in Table 3.1. Plots of the TL ramp and isothermal decay for four different transfer temperatures are shown in Figure 3.4, for SUTL2986/1 following a 200Gy dose. The corresponding plots for SUTL2986/6 are similar, with higher peak photon counts. These plots are qualitatively very similar to corresponding plots for the samples from Vietnam. For the data following the 200Gy dose, the TT-OSL signal is generally larger for both samples than was observed in the samples from Vietnam, with a higher TT-OSL : OSL ratio, in the samples from Vietnam it was observed that a 60s hold temperature was sufficient to deplete the TT-OSL signal to detection limit whereas in these samples this is a significant signal. The observed ID counts here are also significantly larger than observed in the samples from Vietnam, typically 30-50,000 here compared to 6000 from the Vietnam samples. Thus, it appears that a transfer procedure similar to that used for the samples in Vietnam would also be applicable here, with the possibility that the TT-OSL signal will also be usable.

It is noted that the ID and TT-OSL signals, and the TL-ramp to higher temperatures, are generally larger for the natural signal than following the 200Gy dose suggesting that both of these samples have an equivalent dose of at least 200Gy.

Table 3.1: Measured counts for the OSL, TL ramp, ID and TT-OSL for both samples with four transfer temperatures. For the natural signal (top half) and following a 200Gy dose.

Natural						
Sample	Temp	OSL	TL	ID	TT-OSL	TT-OSL:OSL %
2986/1	260	86415 ± 312	7442 ± 95	90106 ± 300	2104 ± 92	2.43 ± 0.11
2986/1	260	52499 ± 254	7451 ± 95	85099 ± 292	1977 ± 90	3.77 ± 0.17
2986/1	280	33107 ± 204	18219 ± 142	76560 ± 277	1424 ± 71	4.3 ± 0.22
2986/1	280	57192 ± 259	18782 ± 145	84341 ± 290	1518 ± 76	2.65 ± 0.13
2986/1	300	32138 ± 203	61432 ± 253	90316 ± 301	545 ± 60	1.7 ± 0.19
2986/1	300	29718 ± 191	37423 ± 200	79178 ± 281	714 ± 60	2.4 ± 0.2
2986/1	320	61323 ± 265	66960 ± 264	81925 ± 286	718 ± 57	1.17 ± 0.09
2986/1	320	45041 ± 234	94540 ± 313	49859 ± 223	731 ± 52	1.62 ± 0.12
2986/6	260	617840 ± 796	6478 ± 89	61199 ± 247	9921 ± 130	1.61 ± 0.02
2986/6	260	691886 ± 843	5926 ± 86	83653 ± 289	15189 ± 159	2.2 ± 0.02
2986/6	280	632091 ± 801	31026 ± 182	54774 ± 234	2360 ± 78	0.37 ± 0.01
2986/6	280	308035 ± 567	30465 ± 180	59654 ± 244	5383 ± 100	1.75 ± 0.03
2986/6	300	1068505 ± 1053	101559 ± 323	135483 ± 368	13158 ± 150	1.23 ± 0.01
2986/6	300	880390 ± 946	85138 ± 296	91798 ± 303	2247 ± 76	0.26 ± 0.01
2986/6	320	606160 ± 791	132455 ± 368	47595 ± 218	1675 ± 68	0.28 ± 0.01
2986/6	320	1061146 ± 1042	121882 ± 353	73351 ± 271	3629 ± 85	0.34 ± 0.01
200 Gy						
2986/1	260	77670 ± 305	10618 ± 111	51395 ± 227	2125 ± 90	2.74 ± 0.12
2986/1	260	73532 ± 305	14184 ± 125	44049 ± 210	1752 ± 92	2.38 ± 0.13
2986/1	280	45942 ± 244	16639 ± 137	32504 ± 180	952 ± 68	2.07 ± 0.15
2986/1	280	66898 ± 289	24986 ± 165	33748 ± 184	1340 ± 79	2 ± 0.12
2986/1	300	43893 ± 239	44731 ± 218	34283 ± 185	452 ± 59	1.03 ± 0.13
2986/1	300	30112 ± 195	29938 ± 181	32912 ± 181	450 ± 57	1.49 ± 0.19
2986/1	320	67312 ± 286	45075 ± 220	33434 ± 183	671 ± 54	1 ± 0.08
2986/1	320	65152 ± 278	48135 ± 227	19170 ± 138	166 ± 48	0.25 ± 0.07
2986/6	260	480244 ± 711	12936 ± 121	45462 ± 213	12592 ± 140	2.62 ± 0.03
2986/6	260	761077 ± 896	12991 ± 120	65240 ± 255	16557 ± 161	2.18 ± 0.02
2986/6	280	386895 ± 629	29575 ± 178	25422 ± 159	1154 ± 68	0.3 ± 0.02
2986/6	280	333863 ± 603	33591 ± 189	31037 ± 176	5913 ± 105	1.77 ± 0.03
2986/6	300	900356 ± 994	104632 ± 328	59360 ± 244	6238 ± 114	0.69 ± 0.01
2986/6	300	603459 ± 790	79145 ± 286	37400 ± 193	1556 ± 68	0.26 ± 0.01
2986/6	320	641189 ± 815	94561 ± 313	24996 ± 158	1071 ± 59	0.17 ± 0.01
2986/6	320	993492 ± 1028	96109 ± 315	34873 ± 187	3420 ± 83	0.34 ± 0.01

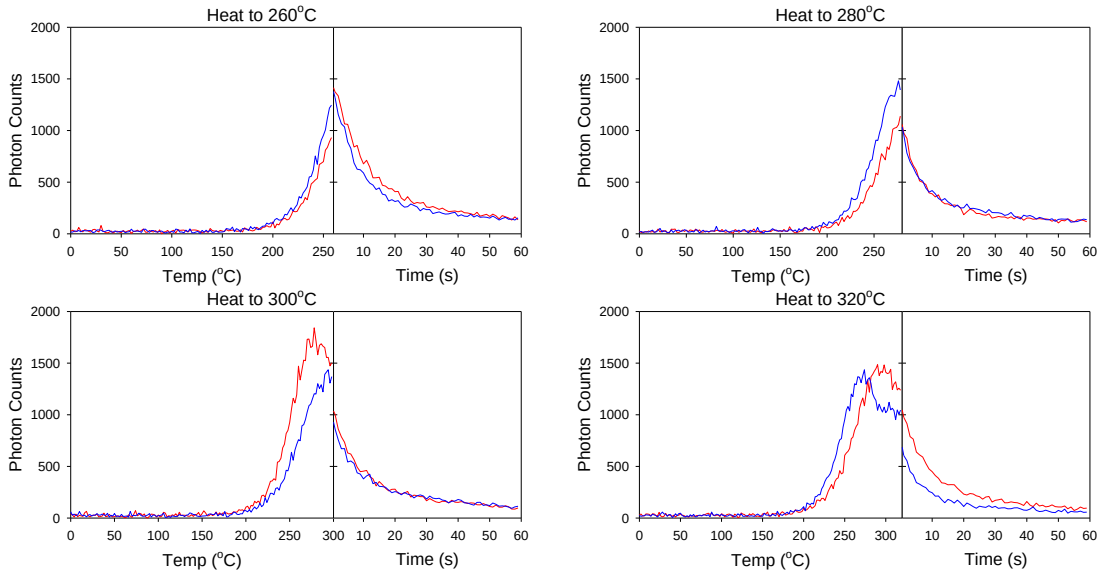

Figure 3.4: TL heating ramp to 260°C, 280°C, 300°C and 320°C with subsequent 60s isothermal decay for pairs of aliquots of SUTL2986/1 after a 200 Gy irradiation.

3.3. Quartz Single Aliquot Regeneration (SAR) and Dose Extension

A procedure to combine Single Aliquot Regeneration (SAR) with dose extension through thermal transfer (see section 2.4.4) was applied to 150-250µm quartz grains extracted from the tube samples. Quality parameters for the OSL SAR measurements (sensitivity and change per cycle, recycling ratio, zero cycle and IR percentage) are given in Table 3.2. The three samples from Kok Yai (SUTL2987 and 2988) and Sa Kaeo (SUTL2990) show high sensitivities (~100000 c Gy^{-1}), with relatively large increases in sensitivity over the SAR sequence (10-25% per cycle). The fourth sample (SUTL2989 from the base of the Huai Om profile) has a sensitivity that is very much lower with no significant change in sensitivity over the SAR sequence, similar to the Hue samples from Vietnam (Cresswell et.al. 2018a). In all cases the photon counts following the zero dose are positive, but small, and recycling ratios are within 10% of unity.

Table 3.2: Quality parameters for OSL SAR measurements to 50 Gy

Sample	Sensitivity c Gy^{-1}	Sensitivity change /cycle %	Zero cycle	Recycling ratio	% IR
SUTL2987	102700 ± 5900	13.3 ± 2.6	0.13 ± 0.01	1.09 ± 0.03	0.4 ± 0.1
SUTL2988	107000 ± 5000	13.1 ± 2.1	0.14 ± 0.02	0.99 ± 0.01	0.4 ± 0.1
SUTL2989	1000 ± 100	-0.6 ± 2.8	0.61 ± 0.11	0.99 ± 0.05	10.7 ± 0.5
SUTL2990	89200 ± 4100	23.7 ± 2.8	0.25 ± 0.02	0.94 ± 0.02	0.4 ± 0.1

Quality parameters for the dose extension measurements (sensitivity, recycling ratio and zero cycle) are reported in Table 3.3. It was observed that the test dose responses for the dose extension measurements carry a residual signal from the regeneration dose, and hence are not reliable measures of sensitivity, hence the TL-ramp, ID and TT-OSL measurements are used without normalisation, and assume no sensitivity change through the measurement cycle (as indicated by the recycling ratios, which for these measurements are calculated as the ratio of counts following the final 50Gy to the counts following the initial 50Gy dose). The sensitivities for these methods are

significantly lower than for the OSL measurements, by up to three orders of magnitude. The samples with high OSL sensitivity have higher sensitivity for the dose extension measurements. The TL-ramp and TT-OSL response to zero dose is generally positive but small, with the uncertainties for the ID zero measurements greater than the measured values. Recycling ratios for the TL-ramp measurements are within 25% of unity, whereas for the other measurements these tend to be larger.

Table 3.3: Quality parameters for dose extension from 50-1000 Gy

Sample	Sensitivity c Gy^{-1}	Zero cycle	Recycling ratio
	TL-ramp		
SUTL2987	103 ± 15	53 ± 16	0.97 ± 0.08
SUTL2988	114 ± 22	54 ± 27	1.14 ± 0.05
SUTL2989	23 ± 5	13 ± 22	1.25 ± 0.15
SUTL2990	148 ± 40	40 ± 26	0.96 ± 0.03
	ID		
SUTL2987	100 ± 15	50 ± 220	0.87 ± 0.08
SUTL2988	128 ± 20	75 ± 225	1.49 ± 0.06
SUTL2989	47 ± 6	90 ± 232	1.26 ± 0.06
SUTL2990	112 ± 15	107 ± 230	1.01 ± 0.04
	TT-OSL		
SUTL2987	402 ± 39	2202 ± 1213	1.28 ± 0.05
SUTL2988	483 ± 102	808 ± 176	1.29 ± 0.09
SUTL2989	13 ± 4	305 ± 233	1.66 ± 0.14
SUTL2990	644 ± 98	1633 ± 488	1.26 ± 0.07

Dose response curves (Appendix B) were fitted through the measured data, from which the equivalent dose that would produce the measured natural signal was determined for each aliquot, for each of the four measurements.

Mean equivalent doses were determined for each sample using an unweighted arithmetic mean, a weighted mean and a robust mean. These are tabulated in Appendix C, with plots of the distributions of equivalent dose. The preferred mean values for each of the measurements are given in Table 3.4. It can be seen that for the samples which do not saturate under SAR OSL (SUTL2987, 2988 and 2990) that the equivalent dose determined from the TL-ramp and TT-OSL tends to be lower than that determined by SAR-OSL by upto 30%, whereas the ID method produces equivalent doses that are 50-80% larger. Direct comparisons between aliquots (Fig. 3.5) shows a similar slope for all three dose extension measurements (0.7-0.8), but with the ID method giving a large positive intercept. Thus, in the low dose region, it appears that the TL-ramp and TT-OSL measurements reproduce the equivalent dose measured by the SAR-OSL method better, albeit underestimating by approximately 20%. On this basis, it is expected that these measurements would be preferred for the sample where the SAR-OSL is saturated (SUTL2989), though potentially underestimating the equivalent dose by approximately 20%.

Table 3.4: Equivalent doses determined for each sample by SAR-OSL and extended dose methods

Sample	Equivalent Dose (Gy)			
	SAR-OSL	TL-ramp	ID	TT-OSL
SUTL2987	10.7 ± 0.5	7.0 ± 0.3	18.6 ± 0.9	7.2 ± 0.7
SUTL2988	8.6 ± 0.1	7.2 ± 0.5	15.8 ± 1.2	7.3 ± 0.8
SUTL2989	>50 Gy	136 ± 5	338 ± 38	105 ± 12
SUTL2990	4.3 ± 0.1	4.4 ± 0.7	6.6 ± 1.4	3.6 ± 0.7

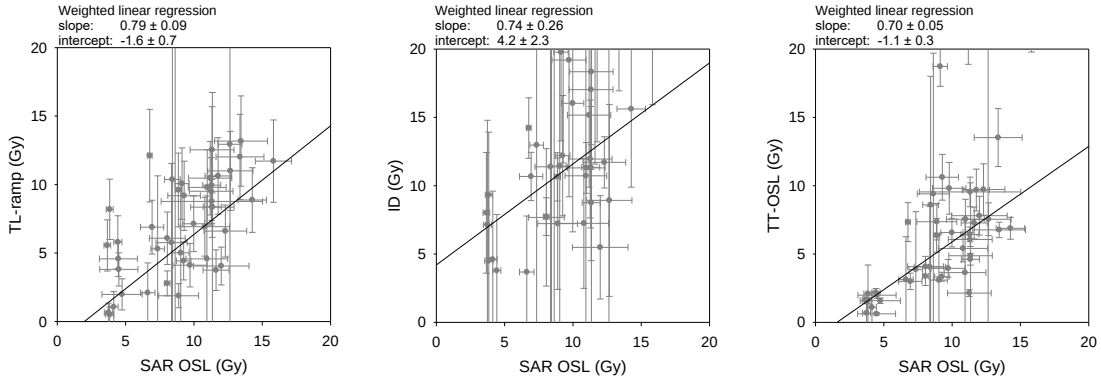

Figure 3.5: Comparison of equivalent doses determined for each aliquot of SUTL2987, 2989 and 2990 using the dose extension measurements and the SAR OSL.

3.4. Dose Rates

HRGS results are shown in Table 3.5, both as activity concentrations (i.e. disintegrations per second per kilogram) and as equivalent parent element concentrations (in % and ppm), based in the case of U and Th on combining nuclide specific data assuming decay series equilibrium.

Table 3.5: Activity and equivalent concentrations of K, U and Th determined by HRGS

SUTL no.	Activity Concentration[a] / Bq kg^{-1}			Equivalent Concentration[b]		
	K	U	Th	K / %	U / ppm	Th / ppm
2987	5 ± 33	26 ± 3	23 ± 2	0.01 ± 0.11	2.1 ± 0.2	5.7 ± 0.5
2988	47 ± 26	21 ± 3	20 ± 2	0.15 ± 0.08	1.7 ± 0.2	5.0 ± 0.5
2989	132 ± 29	27 ± 3	38 ± 2	0.43 ± 0.09	2.1 ± 0.2	9.4 ± 0.6
2990	16 ± 15	11 ± 2	10 ± 2	0.05 ± 0.05	0.9 ± 0.2	2.4 ± 0.4

[a]Shap granite reference, working values determined by David Sanderson in 1986, based on HRGS relative to CANMET and NBL standards.

[b]Activity and equivalent concentrations for U, Th and K determined by HRGS (Conversion factors based on NEA (2000) decay constants): 40K: 309.3 Bq kg^{-1} %K^{-1}, 238U: 12.35 Bq kg^{-1} ppmU^{-1}, 232Th: 4.057 Bq kg^{-1} ppm Th^{-1}

Infinite matrix alpha, beta and gamma dose rates from HRGS are listed for all samples in Table 3.6, together with infinite matrix beta dose rates from TSBC. The gamma spectrometry shows no evidence of disequilibrium in the samples, nor anomalous U:Th ratios, which is supported by the TSBC giving data consistent with the values calculated from the HRGS data. The dry beta dose rates carried forward to calculate effective dose rates are the mean of the HRGS and TSBC values.

Table 3.6: Infinite matrix dose rates determined by HRGS and TSBC

SUTL no.	HRGS, dry[a] / mGy a^{-1}			TSBC, dry / mGy a^{-1}
	Alpha	Beta	Gamma	
2987	10.1 ± 0.7	0.48 ± 0.09	0.54 ± 0.04	0.51 ± 0.04
2988	8.4 ± 0.7	0.52 ± 0.08	0.49 ± 0.04	0.52 ± 0.04
2989	12.9 ± 0.8	0.94 ± 0.09	0.83 ± 0.05	1.02 ± 0.04
2990	4.2 ± 0.6	0.24 ± 0.05	0.24 ± 0.03	0.09 ± 0.03

[a]based on dose rate conversion factors in Aikten (1983), Sanderson (1987) and Cresswell et.al. (2018c)

Effective dose rates to the HF-etched 150-250 μm quartz grains are given in Table 3.7 (the mean of the TSBC and HRGS data, accounting for water content and grain size), together with the estimate of the gamma dose rate (HRGS data, accounting for water content), and the total dose rate (the sum of effective beta and gamma dose rates, and the cosmic dose rate). A cosmic dose rate of 0.185 mGy a^{-1} has been used.

Table 3.7: Effective beta and gamma dose rates following water content correction.

SUTL no.	Water content (%)			Effective Dose Rate / mGy a^{-1}		
	Received	Saturated	Assumed	Beta[a]	Gamma	Total[b]
2987	0.9	19.3	10 ± 10	0.37 ± 0.09	0.48 ± 0.06	1.04 ± 0.11
2988	0.6	16.3	8 ± 8	0.40 ± 0.08	0.45 ± 0.05	1.04 ± 0.09
2989	14.4	17.3	15 ± 2	0.98 ± 0.10	0.72 ± 0.04	1.61 ± 0.08
2990	2.2	20.5	10 ± 10	0.13 ± 0.05	0.21 ± 0.04	0.52 ± 0.06

[a] Effective beta dose rate combining water content corrections with inverse grain size attenuation factors obtained by weighting the 150-250 μm attenuation factors of Mejdahl (1979) for K, U, and Th by the relative beta dose contributions for each source determined by Gamma Spectrometry;
[b] includes a cosmic dose contribution determined by the method of Prescott & Hutton (1994)

4. Discussion

Data from four luminescence studies of the regionally extensive sandy layer across SE Asia have been collated, and summarised below (Table 4.1). These show considerable variability in luminescence sensitivity, dose rates and equivalent doses and dose distributions.

Table 4.1: Summary of dose rates, luminescence properties, equivalent doses and ages for basal samples from four studies of six sites in Thailand and Vietnam.

Location	Dose rate (mGy a^{-1})	OSL intensity (c Gy^{-1})	Equivalent dose (Gy)	Age (ka)	Comment
Khon Kaen, Thailand	1.0 ± 0.1		35 ± 2	35 ± 2	Sanderson et.al. (2001)
Kok Yai, Thailand	0.65 ± 0.03		12.4 ± 2.7	19.2 ± 4.3	Analysis by N. Porat (2017)
Krahad, Thailand	0.67 ± 0.03		5.7 ± 1.0	8.5 ± 1.5	Analysis by N. Porat (2017)
Hue, Vietnam	2.0 ± 0.2	810 ± 90	28 ± 2 (OSL) 200-250 (extended)	14.4 ± 2.1 100-125	Cresswell et.al. (2018a) Cresswell et.al. (2018b)
Kok Yai, Thailand	1.0 ± 0.1	102700 ± 5900	10.7 ± 0.5	10.7 ± 0.5	E_D from SAR-OSL
Huai Om, Thailand	1.6 ± 0.1	1000 ± 100	150 ± 20	95 ± 15	E_D from TL-ramp & TT-OSL, inflated by 20%
Sa Kaeo, Thailand	0.5 ± 0.1	89200 ± 4100	4.3 ± 0.1	8.6 ± 0.2	E_D from SAR-OSL

Four of the sites yield quartz with high luminescence sensitivity, with little dispersion in the equivalent dose determined on multiple aliquots. Equivalent doses determined by SAR OSL on quartz grains from these sites range from 4.3 ± 0.1 Gy (Sa Kaeo), 6 ± 1 Gy (Krahad) to 35 ± 2 Gy (Khon Kaen), with the two studies by different laboratories of the Kok Yai site in good agreement (12 ± 4 and 10.7 ± 0.5 Gy). For those sites where luminescence profiling was conducted (Sa Kaeo, Khon Kaen and Kok Yai) the TL signals produce apparent doses which are similar to the OSL measurements, suggesting significant light exposure prior to deposition resetting both optical and thermal signals. The other two sites yield quartz with luminescence intensities two orders of magnitude lower, in both cases with SAR-OSL resulting in aliquots that saturate (the equivalent doses exceeding the limits of the procedure, greater than 50 Gy). The site at Hue, Vietnam, shows evidence of mixing between younger material (28 ± 2 Gy) and much older material (200-250 Gy). Whereas, at Huai Om there is little evidence of mixing of young and old material with all the aliquots saturating under SAR-OSL, and dose extension methods (TL-ramp and TT-OSL) resulting in relatively narrow dose distributions (150 ± 20 Gy). The laboratory profiling results from Huai Om shows a transition between low and high sensitivity quartz, with the top sample an order of magnitude more sensitive. Whereas profiling measurements from Huai Om show a large residual TL apparent dose suggesting limited light exposure prior to deposition, the profile from Hue shows a low TL apparent dose consistent with the non-saturating OSL equivalent dose (Cresswell et.al. 2018a).

The data from the Portable OSL reader show clear differences between the high and low sensitivity materials, both with at least an order of magnitude difference in OSL intensities (typically ~1000 photon counts for the low sensitivity materials, and ~10,000-100,000 for the high sensitivity) and differences in OSL depletion indices (typically 3.5-4.0 for low sensitivity materials and 4.5-5.5 for the high sensitivity).

Dose rates vary by a factor of four. These materials are generally low in potassium, as observed in the HRGS measurements conducted at SUERC and the ICP-MS/ICP-OES conducted for the Kok Yai and Krahad samples (Porat, 2017) where it was noted that all the Krahad samples and the basal Kok Yai sample had K concentrations below detection limits. The lowest dose rate (0.5 ± 0.1 mGy a^{-1}) is at Sa Kaeo in the south of Thailand. Dose rates for the central and northern areas in Thailand are similar in the range 0.7-1.0 mGy a^{-1}, and higher in SE Thailand at Huai Om (1.6 ± 0.1 mGy a^{-1}). The highest dose rate is at Hue, Vietnam (2.0 ± 0.2 mGy a^{-1}). It is noted that these higher dose rate samples, driven by higher K content at ~0.5%, are also the samples which include quartz with equivalent doses in excess of the OSL-SAR saturation dose (~50Gy).

The data suggests that these sandy layers can be divided into at least two groups. One, sands with ~0.5% K including quartz carrying equivalent doses in excess of 50Gy (saturating OSL-SAR methods). Two, sands with lower (<0.2%) K concentrations and quartz carrying equivalent doses less than 50Gy (not saturating OSL-SAR methods). At Huai Om, both of these are present with the second group overlaying the first implying that these are older, rather than the higher equivalent doses being a result of the higher dose rates and potential residual dose. At Hue, there is evidence that there has been mixing between these groups even at the base of the deposits. At the other sites this older group of materials is absent.

For both Huai Om and Hue, the oldest components have similar ages determined from the dose extension analyses (100 ± 15ka at Huai Om, 100-125ka at Hue). These are significantly younger than the 700-800ka age of the meteorite impact resulting in the tektite gravel layer. The analysis of samples from Hue (Cresswell et.al. 2018b) indicated that the traps responsible for the dose extension measurements may not be thermally stable at environmental temperatures in the region, and thus may produce equivalent doses that have been reduced and ages that are less than the physical ages of these sediments. Preliminary measurements of the trap parameters are insufficient to calculate the appropriate kinetics to determine thermal stability. If the cover sands extend into the mountains in Laos, with elevations over 1000m in places, then samples collected there would have experienced lower environmental temperatures, and if thermal stability is an issue such materials would be less affected.

The ages of the basal layers of the younger group of materials range from 9-18ka (8.6 ± 1.7 ka for Sa Kaeo, 8.5 ± 1.5ka for Krahad and 10.7 ± 1.2ka and 19.2 ± 4.3ka for the two locations at Kok Yai) to 35 ± 4ka at Khon Kaen. For the Huai Om profile, the bottom sample of the overlying high sensitivity material has an apparent dose of 48 ± 1 Gy, which assuming the dose rate is similar to the measured SUTL2989 sample would yield an approximate apparent age of 30 ± 3ka, which is consistent with the age of the basal layer of the high sensitivity material at Khon Kaen. With a factor of four difference in the ages determined for these basal samples in different locations, it appears that either the cover sand deposits were not laid down at the same time across the region, or that in some locations the earlier deposits were removed before later deposition of younger material.

The older material sampled at Huai Om and Hue is significantly younger than the expected dates for material associated with the tektites in the laterite layer. It has been previously noted that the stratigraphic ages of many Australite tektites, dated by K-Ar

methods to 750-800ka, recovered from Australia are around 7-24ka (Lovering et.al. 1972, Chalmers et.al. 1976, 1979, Glass 1978). Glass (1978) notes that in other locations, particularly relevant here within Indochina, the stratigraphic ages of tektites correspond to the K-Ar and fission track ages. Koeberl (1992) notes that Muong Nong-type tektites are sometimes deeply eroded, mainly by interaction with water, thus the paradox of tektites with ages of 750-800ka within much younger sediments could be explained by erosion and re-deposition of the tektites from their original settings into more recent strata.

If the older material dated here to 100-150ka does correspond to the stratigraphic settings for the tektites then this relatively young age could be the result of re-working of the laterites moving tektites into younger strata. Or, as noted (Cresswell et.al 2018b) the traps used to extend the range of equivalent dose measurements may be unstable over ~10^5 year timescales. The stability of these traps can be investigated further. It is noted that these older materials are in samples from Huai Om and Hue, and that there is a mountain range extending to over 1000m in Laos between these locations. If these cover sands extend into this range then samples could be collected which have been exposed to lower environmental temperatures, and hence would give older ages. The Portable OSL results show that this instrument can readily distinguish between the older dim quartz and the younger bright quartz in the field, providing a means to efficiently identify suitable materials.

5. Conclusions

The work reported here suggests there are two groups of material within the cover sands that can be readily distinguished by luminescence methods.

1. A group with lower luminescence sensitivity, and OSL depletion indices of 3.5-4.0 measured on the SUERC Portable OSL instrument, with quartz that carries an equivalent dose beyond the saturation limit of OSL-SAR approaches. This is found in the lower 50cm of the Huai Om profile, and at Hue where it appears to be mixed with younger material.

2. A group with very high luminescence sensitivity, and OSL depletion indices of 4.5-5.5 measured on the SUERC Portable OSL instrument, with quartz that carries readily quantifiable OSL-SAR equivalent doses. This is found in the upper part of the Huai Om profile, at the other sites in Thailand, and appears to be mixed with the older material at Hue. The ages determined for the basal samples, and for the sample from Huai Om immediately above the older (group 1) material range from 9 to 35ka.

Dose extension methods based on thermal transfer from deeper traps have been used to determine equivalent doses for the older (group 1) materials. Applied to group 2 materials, these give equivalent doses within 20% of the OSL method. For the older materials at Huai Om these give equivalent doses of 150 ± 20Gy, and 200-250Gy for Hue. Both of these are consistent with an age of 100-150ka. The luminescence data suggest that the traps associated with these extended dose measurements may have lifetimes of ~10^5 years at environmental temperatures of 25°C, which would result in a significant underestimate of the age of these minerals. Further investigations to determine whether trap stability is an issue are suggested, including (if possible) collection of samples from equivalent contexts at higher altitude where environmental temperatures would be reduced.

The use of OSL intensities and depletion indices from the Portable OSL reader would be a method of rapidly distinguishing between the two groups of sand in the field.

References

Aitken, M.J., 1983, Dose rate data in SI units: PACT, v. 9, p. 69–76.

Bishop, P., Mitchell, P., Paton, T.R., 1980. The formation of duplex soils on hillslopes in the Sydney Basin, Australia. Geoderma 23, 175-189.

Boonsener, M., Tassanasorn, A., 1983. The geomorphology of Quaternary deposits in Khon Kaen Province, northeastern Thailand. In: Thiramongkol, N., Pisutha-Arnond, V. (Eds), Proceedings of the First Symposium on Geomorphology and Quaternary Geology of Thailand (October 28-29, 1983), Deptartment of Geology Chulalongkorn University, Department of Mineral Resources, and Geological Society of Thailand, pp. 106-111.

Boonsener, M., 1987. Quaternary geology of Khon Kaen Province, northeastern Thailand. In: Thiramongkol, N. (Ed.), Proceedings of the Workshop on Economic Geology. Tectonics, Sedimentary Processes and Environment of the Quaternary in Southeast Asia (3-7 February, 1986, Haad Yai, Thailand), International Geological Correlations Programme, Dept of Geology Chulalongkorn University, Association of Geoscientists for International Development, pp. 75-85.

Chalmers, R.O., Henderson, E.P., Mason, B., 1976. Occurrence, distribution, and age of Australian tektites. Smithsonian Contrib. Earth Sci. 17, l-46.

Chalmers, R.O., Henderson, E.P., Mason, B., 1979. Australian microtektites and the stratigraphic age of the australites: Discussion. GSA Bull. 90, 508-5 10.

Cresswell, A.J., Sanderson, D.C.W., Carling, P.A., 2018a. Luminescence Profile Measurements on Samples from Vietnam Submitted by P. Carling. SUERC Technical report.

Cresswell, A.J., Sanderson, D.C.W., Carling, P.A., 2018b, Dose Extension of a Sample at the Base of a Sedimentary Sequence in Vietnam. SUERC Technical Report.

Cresswell, A.J., Carter, J., Sanderson, D.C.W., 2018c, Dose rate conversion parameters: assessment of nuclear data. Radiation Measurements 120, 195-201. doi 10.1016/j.radmeas.2018.02.007

Darwin, C.R., 1844. Geological observations on the volcanic islands visited during the voyage of H.M.S. Beagle, together with some brief notices of the geology of Australia and the Cape of Good Hope. Being the second part of the geology of the voyage of the Beagle, under the command of Capt. Fitzroy, R.N. during the years 1832 to 1836. Smith Elder and Co., London, pp. 36–39.

De Dapper, M., 1987. Landform development during the Late Quaternary in the upland of peninsular Malaysia. In: Wezel, F.W., Rau, J.L. (Eds), Progress in Quaternary Geology of East and Southeast Asia. Proceedings of the CCOP Symposium on Developments in Quaternary Geological Research in E and SE Asia During the Last Decade, (27-30 October, 1986, Bangkok, Thailand), CCOP Technical Publication Vol. 18, pp. 109-134.

Dheeradilok, P., 1987. Review of Quaternary geological mapping and research in Thailand. In: Wezel, F.W., Rau, J.L., (Eds), Proceedings of the CCOP Symposium on Developments in Quaternary Geological Research in East and Southeast Asia During the Last Decade, 27-30 October, 1986, Bangkok, Thailand.

Fleischer, R.L., Price, P.B., Viertl, J.R.M., Woods, R.T., 1969, Ages of Darwin Glass, Macedon Glass, and Far Eastern tektites. Geochimica et Cosmochimica Acta, 33, 1071-1074.

Gentner, W., Storzer, D., Wagner, G.A., 1969, New fission track ages of tektites and related glasses. Geochimica et Cosmochimica Acta, 33, 1075-1081.
Glass, B.P., 1978. Australasian microtektites and the stratigraphic age of the australites. GSA Bull. 89, 1455-1458.
Hoang Ngoc Ky., 1989. The Thu Duc loess formation, a typical aeolian deposit of tropical regions, in ESCAP Secretariat, Quaternary Stratigraphy of Asia and the Pacific. IGCP 296 (1989). ESCAP Atlas of Stratigraphy X (Mineral Resources Development Series 60), pp. 100-104.
Hoang Ngoc Ky., 1994. Stratigraphic correlation of Quaternary transgressional and regressional deposits in Viet Nam and adjacent countries. In: ESCAP Secretariat, Quaternary Stratigraphy of Asia and the Pacific. IGCP 296. ESCAP Atlas of Stratigraphy XIII Mineral Resources Development Series Vol. 63, pp. 141-149.
Johnson, D.L., 1993. Dynamic denudational evolution of tropical, subtropical and temperate landscapes with three tiered soils: toward a general theory of landscape evolution. Quaternary International 17, 67-78.
Koeberl, C., 1992, Geochemistry and origin of Muong Nong-type tektites, Geochimica et Cosmochimica Acta, 56, 1033-1064.
Lacroix, A., 1935. Les tectites sans formes figurées de l'Indochine. Comot. Rend. Acad. Sci. Paris, 200, 2129-2132.
Löffler, E., Kubiniok, J., 1991. The age and origin of the Yasothon soils and associated gravel deposits. Journal of the Geological Society of Thailand 1, 69-74.
Löffler, E., Kubiniok, J., 1996. landform development and bioturbation on the Khorat plateau, northeast Thailand. Natural History Bulletin of the Siam Society 44, 199-216.
Lovering, J.F., Mason, B., Williams, G. E., McColl, D. H., 1972, Stratigraphical evidence for the terrestrial age of australites, Journal of the Geological Society of Australia, 18, 409-418.
Mejdahl, V., 1979, Thermoluminescence daing: Beta-dose attenuation in quartz grains Archaeometry, v. 21, p. 61-72.
Mizera, J., Řanda, Z., Kameník, J., 2016, On a possible parent crater for Australasian tektites: Geochemical, isotopic, geographical and other constraints. Earth-Science Reviews 154, 123–137.
NEA, 2000, The JEF-2.2 Nuclear Data Library: Nuclear Energy Agency, Organisation for economic Co-operation and Development. JEFF Report, v. 17.
Nichol, J.E, Nichol, D.W., 2015, Character and provenance of aeolian sediments in northeast Thailand. Aeolian Research 19, 5–14.
Nguyen Duc Tam, 1994. Review of Quaternary geological studies in Vietnam, in ESCAP Sectretariat, Quaternary Stratigraphy of Asia and the Pacific, IGCP 296. United Nations Mineral Resources Development Series 63, 137-140.
Porat, N., 2017, Thailand Ages Summary (included as Appendix D to this report).
Prescott, J.R., and Hutton, J.T., 1994, Cosmic ray contributions to dose rates for luminescence and ESR dating: Large depths and long-term time variations: Radiation Measurements, v. 23, p. 497-500.
Sanderson, D.C.W., 1987, Thermoluminescence dating of vitrified Scottish Forts: Paisley, Paisley college.
Sanderson, D.C.W., 1988, Thick source beta counting (TSBC): A rapid method for measuring beta dose-rates: International Journal of Radiation Applications and Instrumentation. Part D. Nuclear Tracks and Radiation Measurements, v. 14, p. 203-207.

Sanderson, D.C.W., Bishop, P., Houston, I., Boonsener, M., 2001, Luminescence characterisation of quartz-rich cover sands from NE Thailand. Quaternary Science Reviews 20, 893-900.
Sanderson, D.C.W., and Murphy, S., 2010, Using simple portable OSL measurements and laboratory characterisation to help understand complex and heterogeneous sediment sequences for luminescence dating: Quaternary Geochronology, v. 5, p. 299-305.
Schmidt, G., Zhou, L., Wasson, J.T., 1993. Iridium anomaly associated with the Australasian tektite-producing impact: masses of the impactor and of the Australasian tektites. Geochim. Cosmochim. Acta 57, 4851–4859.
Schnetzler, C.C., Walter, L.S., Marsh, J.G., 1988. Source of the Australasian tektite strewn field: a possible off shore impact site. Geophys. Res. Lett. 15, 357–360.
Shaw, H.F.,Wasserburg, G.J., 1982. Age and provenance of the target materials
Šibrava, V., 1993. Quaternary sequences in Southeast Asia and their regional correlation, in ESCAP Secretariat, Quaternary Stratigraphy of Asia and the Pacific. IGCP 296. ESCAP Secretariat, Quaternary Stratigraphy of Asia and the Pacific. IGCP 296. ESCAP Atlas of Stratigraphy XII (Mineral Resources Development Series 62), pp. 1-29.
Sonsuk, M., Hastings, P., 1984. An age for the Yasothon soils series in the Sakhon Nakhon basin. Journal of the Geological Society of Thailand VII, 1-11.
Tamura, T., 1992. Landform Development and Related Changes in the Chi River Basin, Northeast Thailand. The Science Reports of the Tohoku University, 7th Series, vol 42, 107-127.
Udomchoke, V., 1989. Quaternary stratigraphy of the Khorat Plateau area northeastern Thailand. In: Thiramongkol, N. (Ed.), Proceedings of the Workshop on Correlations of Quaternary Successions in South, East and Southeast Asia (November 21-24, 1988), International Geological Correlation Programme, Chulalongkorn University Dept of Geology, UNESCO Regional Office for Science and Technology SE Asia, ESCAP, 69-94.
Williams, M.A.J., 1978. Termites, soils and landscape equilibrium in the Northern Territory of Australia. In: Davies, J.L., Williams, M.A.J. (Eds.), Landform Evolution in Australasia. ANU Press, Canberra, pp. 128-141.

Appendix A: Portable OSL and Laboratory Profiling Data

Table A.1: Measurements of profile from Huai Om (SUTL2986) using the SUERC Portable OSL instrument.

	IRSL		OSL		
Sample	Net counts	Depletion index	Net counts	Depletion index	IRSL:OSL
SUTL2986/1	14959 ± 135	1.38 ± 0.03	724634 ± 854	3.72 ± 0.01	0.021 ± 0.001
SUTL2986/2	8737 ± 110	1.32 ± 0.03	877935 ± 940	3.87 ± 0.01	0.010 ± 0.001
SUTL2986/3	9536 ± 115	1.42 ± 0.04	698785 ± 839	3.85 ± 0.01	0.014 ± 0.001
SUTL2986/4	9272 ± 120	1.35 ± 0.04	608245 ± 784	3.83 ± 0.01	0.015 ± 0.001
SUTL2986/5	7334 ± 107	1.27 ± 0.04	438459 ± 667	3.69 ± 0.01	0.017 ± 0.001
SUTL2986/6	8774 ± 114	1.43 ± 0.04	9432207 ± 3074	5.17 ± 0.01	0.001 ± 0.001

Table A.2: Laboratory measurements of OSL from nominal quartz grains.

	Sensitivity c/Gy			Sensitivity change			Apparent dose (Gy)		
Sample	Al 1	Al 2	Mean	Al 1	Al 2	Mean	Al 1	Al 2	Mean
SUTL2986/1	3499 ± 130	3169 ± 137	3334 ± 94	0.72 ± 0.04	0.76 ± 0.05	0.74 ± 0.03	59.2 ± 3.5	47.2 ± 3.7	53.2 ± 2.5
SUTL2986/2	5696 ± 151	1881 ± 106	3788 ± 92	0.64 ± 0.03	1.05 ± 0.08	0.85 ± 0.04	34.9 ± 1.8	37.9 ± 4.1	36.4 ± 2.2
SUTL2986/3	2076 ± 108	1194 ± 88	1635 ± 70	0.70 ± 0.06	0.59 ± 0.08	0.64 ± 0.05	50.7 ± 4.1	50.5 ± 6.0	50.6 ± 3.6
SUTL2986/4	1622 ± 94	1227 ± 91	1425 ± 65	0.91 ± 0.08	1.15 ± 0.11	1.03 ± 0.07	45.2 ± 3.8	50.1 ± 5.6	47.7 ± 3.4
SUTL2986/5	2304 ± 104	1822 ± 99	2063 ± 72	1.07 ± 0.06	0.71 ± 0.06	0.89 ± 0.04	27.3 ± 1.9	34.9 ± 3.5	31.1 ± 2.0
SUTL2986/6	26666 ± 224	20087 ± 172	23376 ± 141	0.74 ± 0.01	0.80 ± 0.01	0.77 ± 0.01	56.7 ± 0.7	53.6 ± 0.7	55.1 ± 0.5
SUTL2986/7	13252 ± 136	19570 ± 161	16411 ± 105	0.94 ± 0.01	0.94 ± 0.01	0.94 ± 0.01	0.2 ± 0.1	0.2 ± 0.1	0.2 ± 0.1
SUTL2986/8	25199 ± 201	30823 ± 214	28011 ± 147	0.96 ± 0.01	1.04 ± 0.01	1.00 ± 0.01	0.6 ± 0.1	0.2 ± 0.1	0.4 ± 0.1
SUTL2986/9	137858 ± 402	73166 ± 289	105512 ± 247	0.98 ± 0.01	0.97 ± 0.01	0.97 ± 0.01	0.7 ± 0.1	0.2 ± 0.1	0.4 ± 0.1
SUTL2987	87103 ± 307	57738 ± 264	72420 ± 203	1.14 ± 0.01	1.32 ± 0.01	1.23 ± 0.01	11.2 ± 0.1	10.6 ± 0.1	10.9 ± 0.1
SUTL2988	52806 ± 242	163048 ± 429	107927 ± 247	1.09 ± 0.01	1.20 ± 0.01	1.14 ± 0.01	9.6 ± 0.1	9.2 ± 0.1	9.4 ± 0.1
SUTL2989	378 ± 64	3816 ± 90	2097 ± 55	1.01 ± 0.24	0.68 ± 0.03	0.84 ± 0.12	53.9 ± 14.1	28.5 ± 1.0	41.2 ± 7.1
SUTL2990	58508 ± 261	44982 ± 236	51745 ± 176	1.29 ± 0.01	1.33 ± 0.01	1.31 ± 0.01	8.8 ± 0.1	5.7 ± 0.1	7.2 ± 0.1

Table A.3: Laboratory measurements of OSL from polymineral grains.

	Sensitivity c/Gy			Sensitivity change			Apparent dose (Gy)		
Sample	Al 1	Al 2	Mean	Al 1	Al 2	Mean	Al 1	Al 2	Mean
SUTL2986/1	704 ± 15	223 ± 11	463 ± 9	1.17 ± 0.03	1.14 ± 0.08	1.16 ± 0.04	128.4 ± 1.1	165.5 ± 2.2	147.0 ± 1.2
SUTL2986/2	621 ± 14	631 ± 14	626 ± 10	1.10 ± 0.03	1.30± 0.04	1.20 ± 0.03	93.5 ± 0.9	84.3 ± 0.9	88.9 ± 0.6
SUTL2986/3	506 ± 14	405 ± 13	456 ± 9	1.06 ± 0.04	1.13 ± 0.05	1.09 ± 0.03	117.5 ± 1.1	110.8 ± 1.2	114.1 ± 0.8
SUTL2986/4	410 ± 12	561 ± 14	485 ± 9	1.10 ± 0.05	1.16 ± 0.04	1.13 ± 0.03	132.3 ± 1.3	107.0 ± 1.0	119.6 ± 0.8
SUTL2986/5	348 ± 12	334 ± 12	341 ± 9	1.05 ± 0.05	1.11 ± 0.06	1.08 ± 0.04	105.2 ± 1.3	89.0 ± 1.2	97.1 ± 0.9
SUTL2986/6	15944 ± 58	8782 ± 44	12363 ± 37	1.02 ± 0.01	0.95 ± 0.01	0.98 ± 0.01	131.8 ± 0.3	102.3 ± 0.3	117.0 ± 0.2
SUTL2986/7	6734 ± 38	6027 ± 36	6380 ± 26	0.84 ± 0.01	0.93 ± 0.01	0.88 ± 0.01	0.4 ± 0.1	0.3 ± 0.1	0.4 ± 0.1
SUTL2986/8	53738 ± 105	33533 ± 84	43636 ± 67	1.00 ± 0.01	0.88 ± 0.01	0.94 ± 0.01	0.3 ± 0.1	0.4 ± 0.1	0.3 ± 0.1
SUTL2986/9	150803 ± 178	122071 ± 161	136437 ± 120	1.22 ± 0.01	1.27 ± 0.01	1.24 ± 0.01	0.9 ± 0.1	0.3 ± 0.1	0.6 ± 0.1
SUTL2987	137079 ± 167	128237 ± 163	132658 ± 117	1.50 ± 0.01	1.40 ± 0.01	1.45 ± 0.01	13.6 ± 0.1	10.8 ± 0.1	12.2 ± 0.1
SUTL2988	65975 ± 117	100816 ± 144	83396 ± 93	1.55 ± 0.01	1.43 ± 0.01	1.49 ± 0.01	8.7 ± 0.1	11.1 ± 0.1	9.9 ± 0.1
SUTL2989	1752 ± 20	263 ± 11	1008 ± 12	1.00 ± 0.02	1.24 ± 0.07	1.12 ± 0.04	83.3 ± 0.5	59.3 ± 0.8	71.3 ± 0.5
SUTL2990	40234 ± 94	21162 ± 68	30698 ± 58	1.70 ± 0.01	1.81 ± 0.01	1.75 ± 0.01	16.2 ± 0.1	4.9 ± 0.1	10.6 ± 0.1

Table A.4: Laboratory measurements of IRSL from polymineral grains

	Sensitivity c/Gy			Sensitivity change			Apparent dose (Gy)		
Sample	Al 1	Al 2	Mean	Al 1	Al 2	Mean	Al 1	Al 2	Mean
SUTL2986/1	-5 ± 5	10 ± 5	3 ± 4	-7.36 ± 8.02	0.11 ± 0.58	-3.62 ± 4.02	278.7 ± 26.5	317 ± 43.4	297.8 ± 25.4
SUTL2986/2	19 ± 5	2 ± 6	10 ± 4	1.93 ± 0.62	11.63 ± 42.55	6.78 ± 21.28	432.8 ± 15.4	441.2 ± 40.4	437 ± 21.6
SUTL2986/3	34 ± 5	14 ± 5	24 ± 4	0.81 ± 0.24	0.07 ± 0.45	0.44 ± 0.25	331.5 ± 12.1	319.5 ± 36	325.5 ± 19.0
SUTL2986/4	5 ± 5	4 ± 5	5 ± 4	0.36 ± 1.29	13.95 ± 17.6	7.16 ± 8.82	291.6 ± 32.9	308.6 ± 23.2	300.1 ± 20.1
SUTL2986/5	8 ± 5	13 ± 5	11 ± 4	-0.46 ± 0.82	0.91 ± 0.58	0.22 ± 0.50	315.0 ± 63.6	303.9 ± 97.2	309.5 ± 58.1
SUTL2986/6	9 ± 5	18 ± 5	14 ± 4	1.04 ± 0.90	1.32 ± 0.52	1.18 ± 0.52	292.9 ± 52	132.3 ± 5.9	212.6 ± 26.2
SUTL2986/7	8 ± 5	30 ± 5	19 ± 4	-1.20 ± 1.08	0.08 ± 0.21	-0.56 ± 0.55	-14.0 ± 5.7	-0.2 ± 2.3	-7.1 ± 3.1
SUTL2986/8	16 ± 5	-4 ± 5	6 ± 4	0.90 ± 0.50	-3.11 ± 4.87	-1.11 ± 2.45	-37.2 ± 16.2	-4.2 ± 10.9	-20.7 ± 9.8
SUTL2986/9	17 ± 6	-2 ± 6	8 ± 4	0.10 ± 0.45	-1.27 ± 4.89	-0.58 ± 2.46	11.3 ± 4.6	8.1 ± 3.9	9.7 ± 3.0
SUTL2987	8 ± 6	-14 ± 6	-3 ± 4	1.13 ± 1.18	0.49 ± 0.50	0.81 ± 0.64	20.6 ± 5.2	11.5 ± 5.2	16.1 ± 3.7
SUTL2988	55 ± 6	3 ± 6	29 ± 4	0.47 ± 0.13	5.25 ± 10.24	2.86 ± 5.12	0.8 ± 1.2	106.7 ± 146.1	53.7 ± 73.0
SUTL2989	-8 ± 4	14 ± 5	3 ± 3	2.48 ± 1.55	0.27 ± 0.36	1.37 ± 0.80	149.5 ± 22.4	184.7 ± 60.0	167.1 ± 32.0
SUTL2990	8 ± 5	18 ± 5	13 ± 4	-0.21 ± 0.74	0.59 ± 0.35	0.19 ± 0.41	-1.3 ± 37.5	1.9 ± 9.7	0.3 ± 19.4

Table A.5: Laboratory measurements of TL from polymineral grains

	Sensitivity c/Gy			Sensitivity change			Apparent dose (Gy)		
Sample	Al 1	Al 2	Mean	Al 1	Al 2	Mean	Al 1	Al 2	Mean
SUTL2986/1	662 ± 11	472 ± 10	567 ± 7	0.833 ± 0.021	0.953 ± 0.028	0.893 ± 0.018	528.9 ± 2.7	596.9 ± 3.9	562.9 ± 2.4
SUTL2986/2	425 ± 9	380 ± 9	402 ± 6	1.110 ± 0.033	0.974 ± 0.032	1.042 ± 0.023	639.4 ± 3.8	600.5 ± 3.9	619.9 ± 2.7
SUTL2986/3	682 ± 12	743 ± 12	713 ± 8	0.965 ± 0.023	0.788 ± 0.019	0.877 ± 0.015	575.9 ± 2.6	567.0 ± 2.8	571.5 ± 1.9
SUTL2986/4	517 ± 10	510 ± 10	514 ± 7	0.831 ± 0.024	0.913 ± 0.026	0.872 ± 0.018	590.0 ± 3.3	562.2 ± 3.1	576.1 ± 2.2
SUTL2986/5	443 ± 9	285 ± 8	364 ± 6	0.883 ± 0.027	0.958 ± 0.036	0.920 ± 0.023	562.5 ± 3.2	531.1 ± 3.7	546.8 ± 2.4
SUTL2986/6	1005 ± 14	1129 ± 15	1067 ± 10	1.275 ± 0.024	0.935 ± 0.018	1.105 ± 0.015	411.3 ± 1.8	392.8 ± 1.5	402.0 ± 1.2
SUTL2986/7	1125 ± 15	1476 ± 17	1301 ± 11	0.969 ± 0.018	0.983 ± 0.016	0.976 ± 0.012	143.3 ± 0.6	116.8 ± 0.4	130.1 ± 0.4
SUTL2986/8	1498 ± 17	2399 ± 22	1948 ± 14	0.787 ± 0.014	0.609 ± 0.009	0.698 ± 0.008	102.3 ± 0.5	73.3 ± 0.4	87.8 ± 0.3
SUTL2986/9	5630 ± 33	5550 ± 33	5590 ± 24	0.812 ± 0.007	1.169 ± 0.010	0.991 ± 0.006	34.4 ± 0.1	28.4 ± 0.1	31.4 ± 0.1
SUTL2987	2816 ± 24	3591 ± 27	3203 ± 18	1.323 ± 0.015	1.267 ± 0.013	1.295 ± 0.010	11.4 ± 0.1	11.2 ± 0.1	11.3 ± 0.1
SUTL2988	2509 ± 22	3119 ± 25	2814 ± 17	1.457 ± 0.017	1.392 ± 0.015	1.425 ± 0.011	9.2 ± 0.1	8.7 ± 0.1	9.0 ± 0.1
SUTL2989	386 ± 9	388 ± 9	387 ± 6	0.881 ± 0.029	0.877 ± 0.029	0.879 ± 0.021	413.5 ± 2.8	358.6 ± 2.4	386.1 ± 1.9
SUTL2990	1082 ± 15	964 ± 14	1023 ± 10	1.954 ± 0.032	1.912 ± 0.034	1.933 ± 0.023	6.2 ± 0.1	1.8 ± 0.1	4.0 ± 0.1

Appendix B: Dose response curves

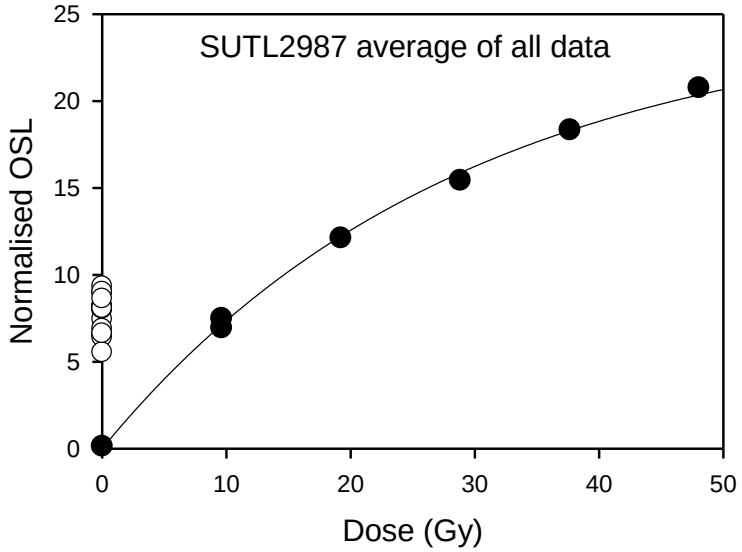

Figure B.1: Dose response curve for OSL SAR measurements on SUTL2987, average of 16 aliquots, with natural signals indicated by open symbols on the left hand axis.

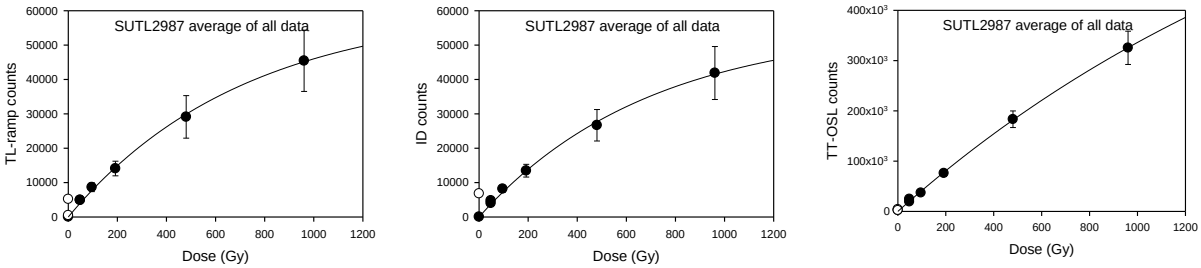

Figure B.2: Dose response curves for dose extension measurements on SUTL2987, average of 12 aliquots (280°C PH group excluded), for the TL-ramp (left), isothermal decay (centre) and TT-OSL (right), with natural signals indicated by open symbols on the left hand axes.

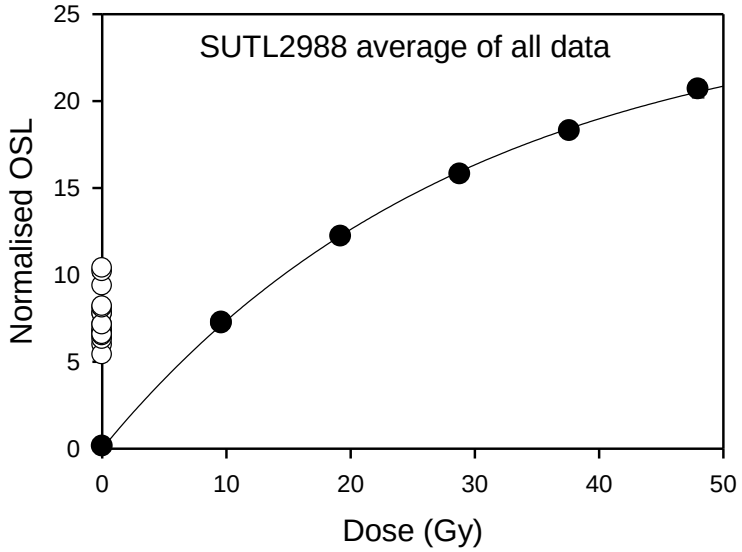

Figure B.3: Dose response curve for OSL SAR measurements on SUTL2988, average of 16 aliquots, with natural signals indicated by open symbols on the left hand axis.

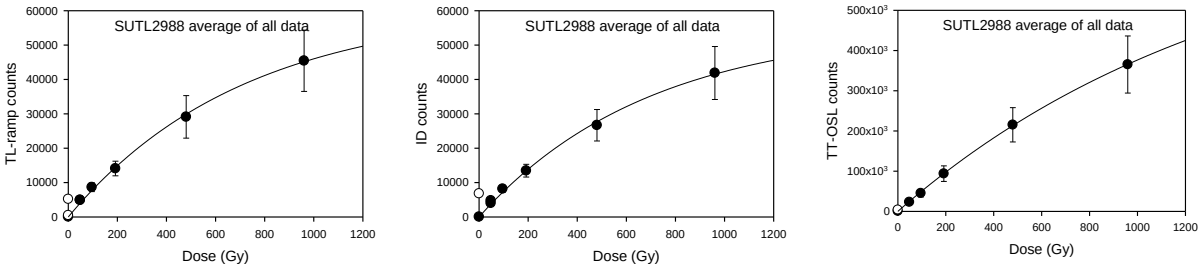

Figure B.4: Dose response curves for dose extension measurements on SUTL2988, average of 12 aliquots (280°C PH group excluded), for the TL-ramp (left), isothermal decay (centre) and TT-OSL (right), with natural signals indicated by open symbols on the left hand axes.

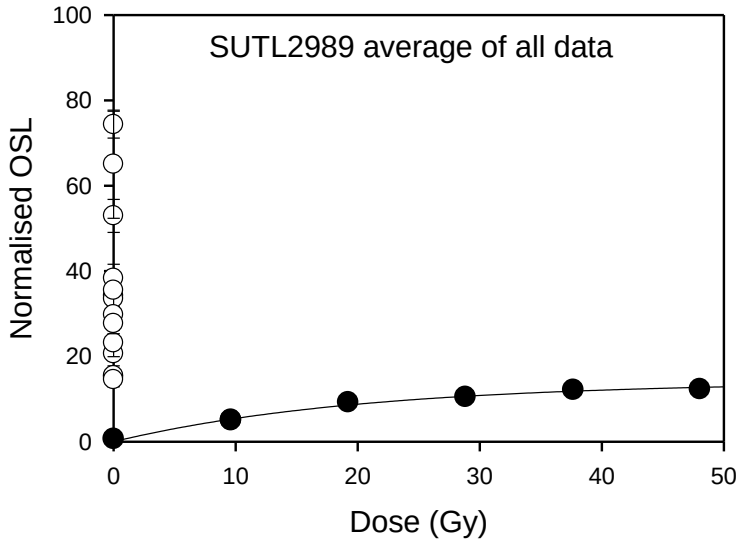

Figure B.5: Dose response curve for OSL SAR measurements on SUTL2989, average of 14 aliquots, with natural signals indicated by open symbols on the left hand axis.

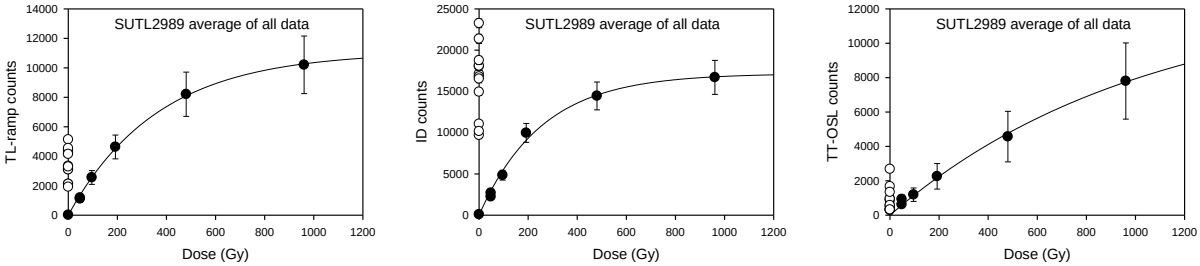

Figure B.6: Dose response curves for dose extension measurements on SUTL2989, average of 12 aliquots (280°C PH group excluded), for the TL-ramp (left), isothermal decay (centre) and TT-OSL (right), with natural signals indicated by open symbols on the left hand axes.

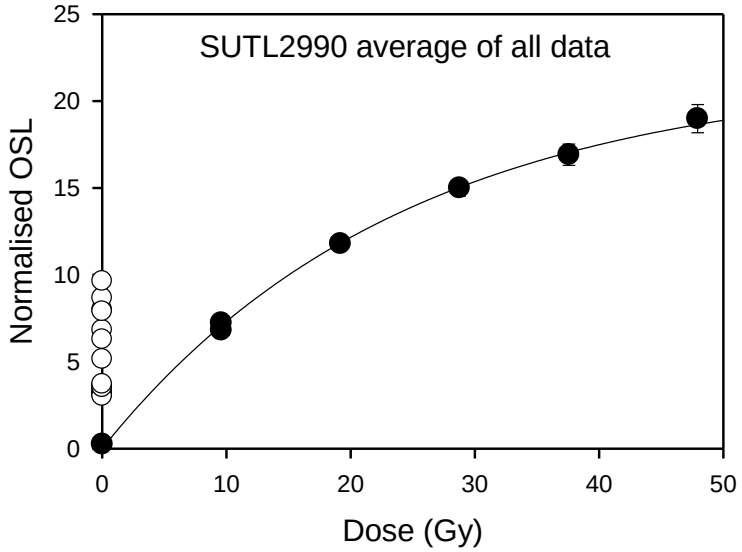

Figure B.7: Dose response curve for OSL SAR measurements on SUTL2990, average of 16 aliquots, with natural signals indicated by open symbols on the left hand axis.

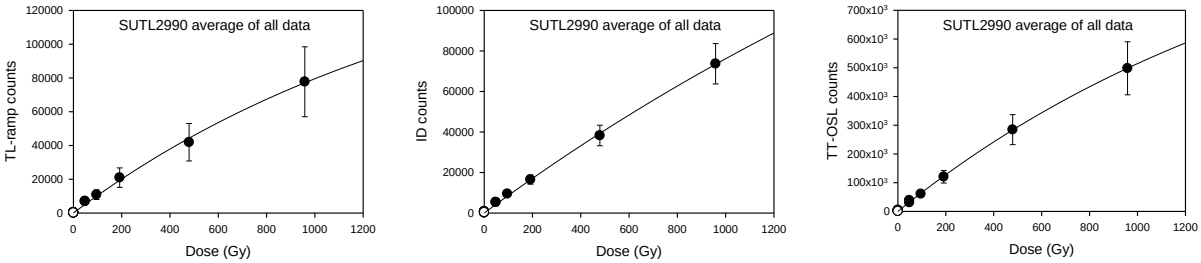

Figure B.8: Dose response curves for dose extension measurements on SUTL2990, average of 16 aliquots, for the TL-ramp (left), isothermal decay (centre) and TT-OSL (right), with natural signals indicated by open symbols on the left hand axes.

Appendix C: Dose distributions

Table C.1: Mean equivalent doses determined by OSL SAR measurements (0-50Gy), preferred value in bold.

Sample	Description of distribution	Mean Equivalent Doses (Gy)		
		Mean	Weighted mean	Robust mean
SUTL2987	Single peak centred at ~11Gy (Fig. C.1)	**10.7 ± 0.5**	10.0 ± 0.4	10.8 ± 0.1
SUTL2988	Three high precision aliquots dominate 7-10Gy dose range, with further peaks at ~12 and ~14Gy (Fig. C.3)	10.4 ± 0.6	**8.6 ± 0.1**	10.2 ± 0.1
SUTL2989	All 14 aliquots satisfying SAR quality criteria have natural signals in excess of the saturation value	**>50Gy**		
SUTL2990	Peak at ~4Gy from 9 out of 16 aliquots, secondary peak ~7Gy and tail to ~17Gy	6.8 ± 0.9	**4.3 ± 0.1**	6.7 ± 0.2

Table C.2: Mean equivalent doses determined by TL-ramp measurements (0-1000Gy), preferred value in bold.

Sample	Description of distribution	Mean Equivalent Doses (Gy)		
		Mean	Weighted mean	Robust mean
SUTL2987	Two peaks at ~6Gy and 11Gy with a tail to higher doses (Fig. C.2)	11.2 ± 2.0	**7.0 ± 0.3**	9.6 ± 0.2
SUTL2988	Broad peak from ~2-11Gy (Fig. C.4). High dose aliquot (280 ± 28Gy) excluded from means.	**7.2 ± 0.5**	6.1 ± 0.3	7.3 ± 0.1
SUTL2989	One saturated (>1000Gy) aliquot. Two peaks in distribution at ~110Gy and ~185Gy, long tail beyond 500Gy (Fig. C.5)	211 ± 41	**136 ± 5**	201 ± 12
SUTL2990	Broad peak ~1-7Gy	**4.4 ± 0.7**	2.4 ± 0.3	4.4 ± 0.2

Table C.3: Mean equivalent doses determined by ID measurements (0-1000Gy), preferred value in bold.

Sample	Description of distribution	Mean Equivalent Doses (Gy)		
		Mean	Weighted mean	Robust mean
SUTL2987	Broad peak 10-30Gy with long tail to higher doses (Fig. C.2)	25.9 ± 2.9	**18.6 ± 0.9**	25.4 ± 0.4
SUTL2988	Broad peak from ~10-20Gy (Fig. C.4). High dose aliquot (430 ± 45Gy) excluded from means.	**15.8 ± 1.2**	14.3 ± 0.7	15.0 ± 0.4
SUTL2989	Five saturated (>1000Gy) aliquots. Slight peak at ~300Gy with long tail beyond 500Gy (Fig. C.5)	502 ± 49	**338 ± 38**	460 ± 54
SUTL2990	Very broad peak centred ~7Gy	7.0 ± 0.8	**6.6 ± 1.4**	6.6 ± 0.2

Table C.4: Mean equivalent doses determined by TT-OSL measurements (0-1000Gy), preferred value in bold.

Sample	Description of distribution	Mean Equivalent Doses (Gy)		
		Mean	Weighted mean	Robust mean
SUTL2987	Peaks in pdf at ~5Gy, 8Gy and ~12Gy (Fig C.2)	**7.2 ± 0.7**	6.1 ± 0.2	6.9 ± 0.1
SUTL2988	Broad peak from ~2-10Gy (Fig. C.4). High dose aliquot (68 ± 7Gy) excluded from means.	**7.3 ± 0.8**	5.7 ± 0.2	6.8 ± 0.1
SUTL2989	Broad peak centred ~100Gy. (Fig. C.5)	109 ± 13	**105 ± 12**	104 ± 2
SUTL2990	Narrow peak at ~2Gy, second broader peak at ~7Gy	**3.6 ± 0.7**	1.3 ± 0.1	3.5 ± 0.2

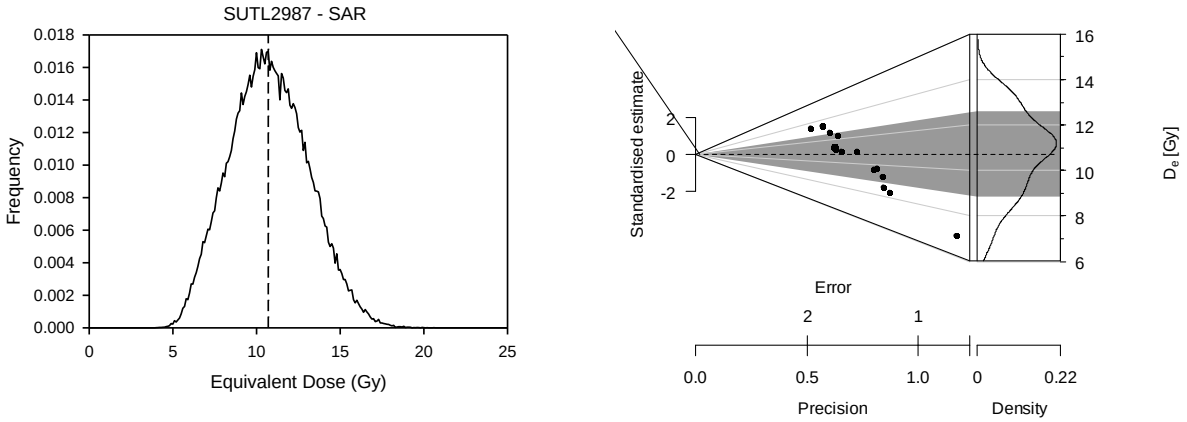

Figure C.1: Probability Density Function (left) and abanico plot (right) for SUTL2987 from OSL SAR measurements, with the mean value indicated.

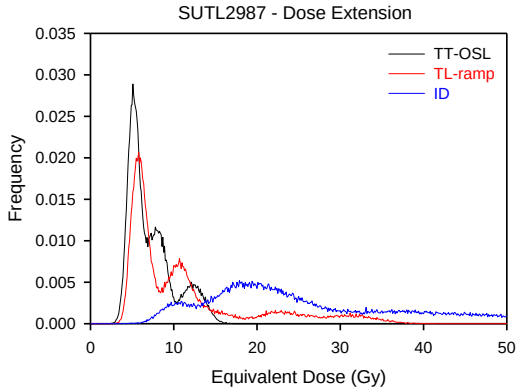

Figure C.2: Probability Density Function for the three measurements of thermally transferred signals for SUTL 2987.

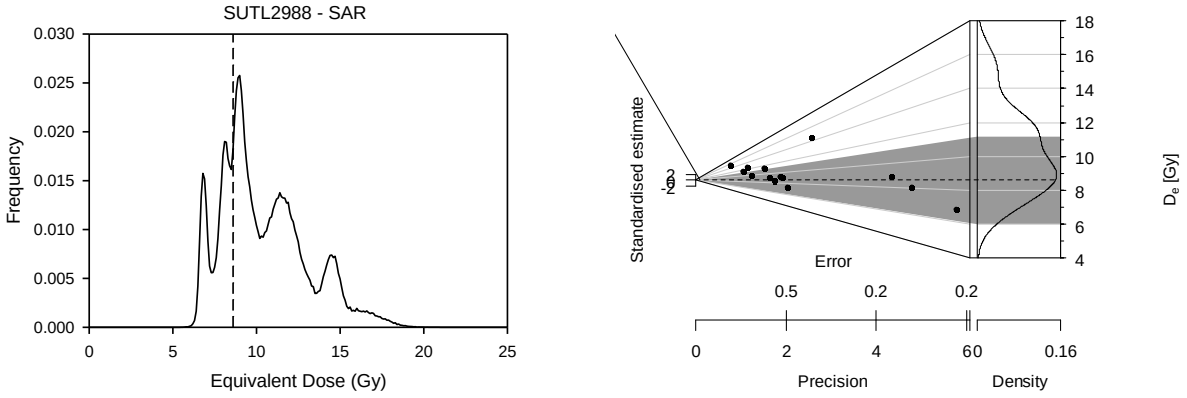

Figure C.3: Probability Density Function (left) and abanico plot (right) for SUTL2988 from OSL SAR measurements, with the weighted mean value indicated.

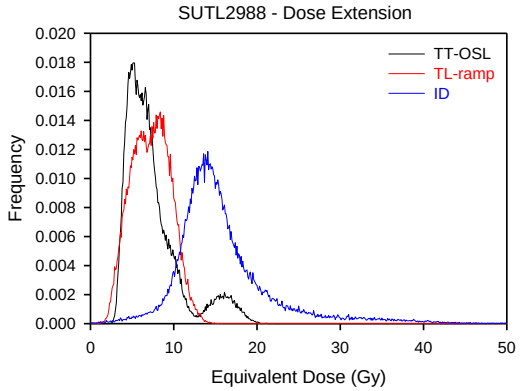

Figure C.4: Probability Density Function for the three measurements of thermally transferred signals for SUTL 2988.

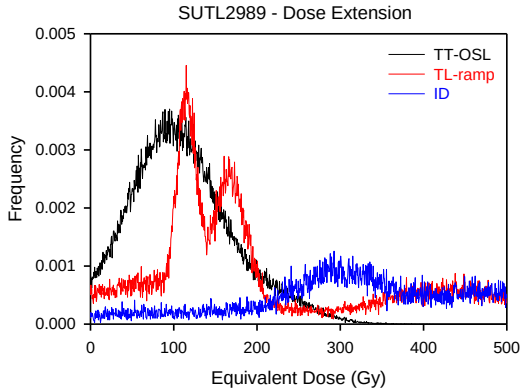

Figure C.5: Probability Density Function for the three measurements of thermally transferred signals for SUTL 2989.

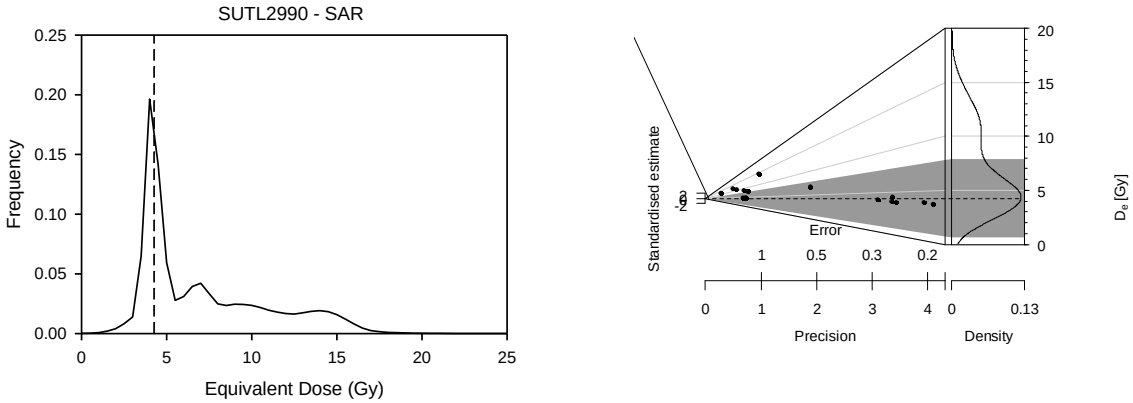

Figure C.6: Probability Density Function (left) and abanico plot (right) for SUTL2990 from OSL SAR measurements, with the weighted mean value indicated.

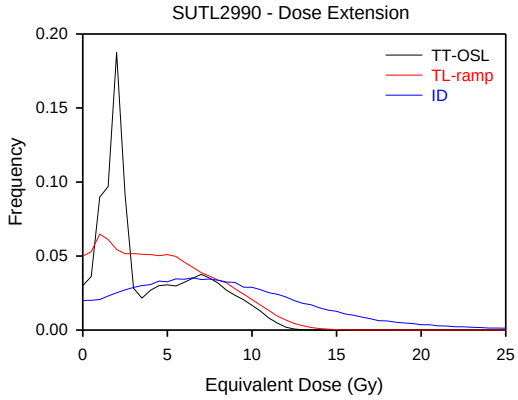

Figure C.7: Probability Density Function for the three measurements of thermally transferred signals for SUTL 2989.

Appendix D: Thailand ages summary (N. Porat, 2017)

Field code	Lab code	Depth (m)	Dose rate (μGy/a)	Aliquots used	OD (%)	De (Gy)	Age (ka)
Krahad							
KRAHAD-1	TAI-3	1.8	670±28	17/19	22	5.7±1.0	8.5±1.5
KRAHAD-2	TAI-4	1.5	854±37	17/19	21	7.7±0.9	9.0±1.1
KRAHAD-3	TAI-5	1.1	859±36	19/19	18	7.0±1.3	8.1±1.6
Kokyai							
KOKYAI-1	TAI-6	1.7	645±27	19/19	21	12.4±2.7	19.2±4.3
KOKYAI-2	TAI-7	1.4	846±37	19/19	22	10.3±2.5	12.2±3.0
KOKYAI-3	TAI-8	0.8	876±37	18/19	20	6.5±1.0	7.5±1.2

Methods:
90-125 μm quartz was purified by wet-sieving to the selected grain size, dissolving carbonates by 8% HCl, removing heavy minerals and most feldspars by magnetic separation, and dissolving the remaining feldspars and etching the quartz with 40% HF (for 40 min), followed by soaking in 16% HCl overnight to dissolve any fluorides which may have precipitated.
Samples were measured using a preheat of 10s @ 260 ^{o}C, a test dose of ~4.6 Gy and a test dose preheat of 5 s @ 240 ^{o}C. Moisture contents were estimated as 20±5 % and density at 1 g/cm^{3}.
De was measured on 2 mm aliquots using a modified single aliquot regenerative (SAR) protocol. All samples show recycling ratios within 4% of unity and negligible IR depletion ratios.
The average De and errors were calculated using unweighted mean.
Alpha, beta and gamma dose rates were calculated from the radioactive elements measured by ICP MS (U&Th) or ICP-OES (K).
For samples TAI-3-6, K contents were below detection limit and a value of 0.08±0.01 was used. An effort should be made to measure K by NAA, as measurable lower values would increase the ages. For example, decreasing K-content for sample TAI-3 to 0.07 increases the age by 100 years.
Cosmic dose rates were estimated from the current burial depths.
OD – Overdispersion.
Aliquots used – the number of aliquots used for the average De out of the aliquots measured.

Naomi Porat, GSI, September 2017.